AN INVESTIGATION INTO AN IMPROVED METHOD OF DEWATERING FINE COAL

Marco le Roux, B.Eng (Minerals)

Dissertation submitted in fulfilment of the requirements for the degree Magister in Engineering at the School of Chemical and Minerals Engineering at the Potchefstroom Uiversity for Christian Higher Education

Supervisor: Mr. Q.P. Campbell

Co-Supervisor: Mr. J.S. de Korte

Potchefstroom

2003

DECLARATION

I, MARCO LE ROUX, hereby declare that the dissertation entitled: AN INVESTIGATION INTO AN IMPROVED METHOD OF DEWATERING FINE COAL, which is done for the completion of the degree Magister in Engineering, is my own work and has never been submitted to any other university.

_____

Marco le Roux

ABSTRACT

Dewatering coal, and especially fine coal (-600μm), is a significant problem in the preparation of coal. The final moisture level of fine coal can be anything up to 30% by weight, depending on the type of dewatering equipment used. Moisture in coal can cause many problems, for example by increasing the transportation costs, as well as decreasing the calorific value of the coal. In industry today there is a need for a dewatering technique that will produce a drier final product.

It was found that an interruption in the application of vacuum during a single dewatering cycle yielded a filter cake with a lower final moisture content. It was also demonstrated that the rate at which the coal is being dewatered is much higher than during continuous vacuum application.

A further study of this phenomenon showed a twofold time dependency involving both the duration of the vacuum break, and the instant it is introduced in the dewatering cycle. An optimum was found at about 29s time duration and an introduction time of 30s, after the start of the cycle.

The possibilities of diffusion and cake structural changes were investigated. For the diffusion tests, repeated interruptions of the vacuum were performed during a single dewatering cycle. Although the kinetics agreed with what was expected, the final moisture content was not as low as that found for the optimum single break test. The compressibility of a coal filter cake was one of the structural changes investigated, the other being an increase in area and, thus, airflow through the cake. Coal filter cakes were shown to be largely incompressible. It was, however, shown that an increase in area, and thus an increase in the airflow through the cake, gave excellent results. An increased area resulted in a much lower final moisture content as well as an increase in the dewatering rate.

The addition of a cake surface cutter to a standard vacuum belt filter will make the application of these finfings relatively easy to industry.

OPSOMMING

Die ontwatering van steenkool, en spesifiek fyn steenkool (-600µm), is tans ‘n groot probleem. Die finale voginhoud van fyn steenkool kan tot soveel as 30% wees, afhangende van die tipe ontwateringstoerusting wat gebruik is. Vog in steenkool kan verskeie probleme tot gevolg hê, byvoorbeeld sal dit die vervoerkoste van die steenkool verhoog, terwyl dit ‘n verlaging in die kaloriewaarde van die steenkool veroorsaak. In die industrie is daar tans ‘n groot aanvraag na tegnieke om ‘n droër finale steenkoolproduk te lewer.

Daar is gevind dat a breek van die toegepaste vakuum gedurende ‘n normale ontwateringsiklus ‘n produk sal lewer met ‘n laer voginhoud. Ook was die tempo van ontwatering veel hoër as by kontinue vakuumtoepassing.

‘n Verdere studie het getoon dat die breek van die vakuum ‘n tweevoudige tydafhanklikheid toon. Dit hang af van beide die tydsduur van die breek en van die brekingstydstip in die ontwateringsiklus. ‘n Optimum is gevind vir ‘n tydsduur van 30s en ‘n tydstip van 29s.

Om hierdie verskynsel te verklaar, is ondersoek ingestel na beide diffusie van water en struktuurveranderinge in die filterkoek. Vir die diffusietoets is herhaalde vakuumonderbrekings in een ontwateringsiklus geimplimenteer. Resultate het die verwagte kinetika getoon, maar het nie dieselfde persentasie verbetering in die finale voginhoud getoon wat die optimale enkelbreuk getoon het nie. Tydens die struktuurveranderingstoetse is getoon dat ‘n steenkool-filterkoek nie saampersbaar is nie. Daar is wel getoon dat ‘n vergroting in die oppervlak van die koek wat blootgestel word aan vakuum, en dus ‘n verhoging in die lugvloei deur die koek, ‘n uitstekende persentasie verlaging in voginhoud toon. Die tempo van ontwatering tydens vergroting van die oppervlak, was ook veel hoër as by vorige toetse.

Deur die aambring van ‘n snyer aan bestaande vakuumfilters, kan hierdie bevindings maklik in die industrie toegepas word.

ACKNOWLEDGEMENTS

I would like to thank the following people and organisations for their help and contributions in the execution of this project. Without their help, what was accomplished, would not have been possible:-

- First of all, many thanks must go to my mentor and supervisor **Mr. Q.P. Campbell** for his guidance, the inputs he made, and for the joy he shared with each new step we took.

- Thanks are also due to **Mr. Dave Tudor** and **Mr. Johan de Korte** of **Coaltech 2020** for the insight they provided during discussions and for believing in me.

- **Ms. Danelle Vorster** of **New Vaal Collieries** always helped and promptly supplied everything needed.

- I would like to thank the staff of Potchefstroom University, School for Chemical and Minerals Engineering for the help I received in setting up the experimental equipment, and for the maintenance done on it.

- Special word of thanks go to the following people for the moral support during this project. Firstly to **Karlé Baumgarten** for always being there to give me a loving smile when things went a bit rough. To **André Mans**, with whom I shared an office for the past two years. Your help and insights are always valuable to me. Thank you for all of that. Finally to my **family** who supported me during this time. I love you all.

- Finally, and most importantly, all that was done would not have been possible without the guidance of my creator and saviour, **God**, in whom my strength lies.

CONTENTS

LIST OF SYMBOLS

A	-	Filter cake area (m^2)
A,B,C	-	Constants
C_c	-	Mass of solids deposited as filter cake per unit volume (kg/m^3)
C_I	-	Mass of solids per unit volume in the feed slurry (kg/m^3)
d_K	-	Kozeny diameter (m)
f_b	-	Modified friction factor
G	-	Gibbs free energy (kJ/kg)
H	-	Enthalpy (kJ/kg)
K	-	Cake permeability (m^2)
K_{ri}	-	Relative permeability (m^2)
L	-	Cake thickness (m)
M_c	-	Mass of the filter cake (kg)
M_{cd}	-	Cake mass after thermal drying (g)
M_{cw}	-	Cake mass after drying (g)
M_f	-	Mass filtrate (g)
M_{fc}	-	Mass filtrate as read from the computer (kg)
M_s	-	Mass solids (g)
M_w	-	Mass water pulled from the cake after 100% saturation (g)
M_{we}	-	Mass of the wet cake (kg)
n	-	Number of moles
P	-	Applied vacuum or pressure (Pa)
P_b	-	Modified threshold pressure / Breakthrough pressure (Pa)
P_T	-	Threshold pressure (Pa)
P_i^*	-	Partial pressure (Pa)
ΔP	-	Pressure difference (Pa)
ΔP_f	-	Filtrate pressure drop (Pa)
ΔP_m	-	Pressure drop across the filter medium (Pa)
R	-	Universal gas constant
Re_p	-	Reynolds number of particles
S	-	Saturation of a filter cake

S - Molar entropy (kJ/kg)

S_E - Equilibrium saturation

S_p - Surface area of a particle (m^2)

S_R - Dimensionless saturation

S_{RE} - Equilibrium dimensionless saturation

S_0 - Specific surface (m^2)

S_∞ - Irreducible saturation

T - Temperature (K)

t - Time (s)

V - Volume (m^3)

V_f - Total volume filtrate (m^3)

V_i - Relative volumetric flux density

V_i^* - Relative partial volume (m^3)

V_p - Particle volume (m^3)

Greek symbols

α - Specific cake surface (m^2)

β - Coal/water contact angle (degrees)

γ - Air/liquid interface tension ($N.m^{-1}$)

ε - Porosity

η - Viscosity of the filtrate (Pa.s)

θ - Dimentionless time

λ - Pore size distribution index

μ - Viscosity (Pa.s)

ν_s - Superficial velocity ($m.s^{-1}$)

ρ - Medium density ($kg.m^{-3}$)

ρ_l - Filtrate density ($kg.m^{-3}$)

Ω_m - Medium resistance

ω - Breakthrough pressure constant

Superscripts

l	-	Liquid
sat	-	Vapour
v	-	Vapour
α,β	-	Phases

Subscripts

a	-	Air
L	-	Liquid
s	-	Solids
∞	-	Irreducible

CD-CONTENTS

The large amount of information gatherd during this investigation is contained in a CD which is included as part of this dissdertation. It also contains the following relavant information:

- Information on the author
- The complete dissertation
- The experimental setup with complete picture gallery
- The complete experimental results
- Additional experimental work that was done
- Photo gallery
- Contact details
- Links to filtration websites.

LIST OF FIGURES

LIST OF TABLES

CHAPTER 1

INTRODUCTION

This chapter will provide a brief introduction to the insights relevant to the motivation and the scope of this project. The project objectives will also be stated.

1.1 Introduction and motivation

Throughout the years the dewatering of fine coal and coal refuse has been problematic. Avoiding the use of water in coal washing plants is not possible. Water is as much part of a coal washing plant, as the dense media used in drums and cyclones.

The dewatering of coal is therefore a problem that needs to be confronted. The question that remains is: 'how'? Many factors need to be considered, and include the quality of the coal, the size of the coal, the economic feasibility and the time required for dewatering.

This led to the development and application of a variety of dewatering equipment (Kelly & Spottiswood, 1997:343-366). Examples of such equipment are dewatering screens, vacuum- and pressure filters, centrifuges and thermal drying equipment. Table 1.1 shows the relation between the efficiency of each piece of equipment and the operating costs, with 1 indicating excellent and 5 indicating poor. It is evident that greater efficiency leads to higher cost of coal dewatering.

Table 1.1 – Comparison of efficiency and operating costs.

Equipment	Efficiency rating	Operating costs rating
1. Dewatering screens	5	1
2. Vacuum filters	3	2
3. Pressure filters	2	3
4. Centrifuges	3	2
5. Thermal drying	1	5

Since the main objective of any plant is profit-making, great care is required in selecting the right equipment. Vacuum filters and screen bowl centrifuges are the most popular for dewatering fine coal. Vacuum filtration will therefore be considered in this dissertation.

In the past, fine coal (defined as –600μm) as well as coal refuse were discarded. New process equipment led to the production of even greater amounts of fine coal until a stage was reached where it became uneconomical to discard the fine coal (Rong & Hitchins, 1994:293-309). Fine coal needed to be dewatered and sold together with the coarser lumps. In a study that was conducted to stress the importance of fine coal dewatering, it was discovered that even a 1 percent moisture decrease in three million tons of clean coal may lead to a US$300,000 saving in transport costs (Tao, Groppo & Parekh, 2000:163-171). With the current exchange rate at roughly R9 = US$1, this is a saving of R2.7 million. This is enough motivation to seriously consider the problem of fine coal dewatering.

1.2 Objectives

The following objectives were to be achieved in executing this project:

1) The first objective was to verify previous results. It had previously been found that if the applied vacuum was released back to atmospheric level during

dewatering tests, the final moisture content was much lower and the rate of dewatering faster (Le Roux, 2000: 1-81).

2) This phenomenon needed to be quantified in the laboratory. The break in applied vacuum would be implemented at different stages of the dewatering process and for various time periods.

3) A possible explanation for the phenomenon was still lacking and the aim was therefore to establish the mechanism involved.

4) The main aim of this project was to consider the different ways in which the new technology could be introduced into industry.

To meet these objectives, it was decided to set a scope for the investigation.

1.3 Scope of investigation

1) To design, build and test a fully computerised bench scale filter.

2) With the results of Le Roux (2000: 1-81) in mind, and by using coal from New Vaal Collieries the influence of the interruption in applied vacuum would be quantified. The test would emulate the dewatering process at New Vaal. Breaks in vacuum would be implemented at different points in a dewatering cycle, and for different lengths of time.

3) The preliminary step would be to try and give an explanation for the previous observations by doing extended experimental work and evaluating certain pre-conceived ideas. If a reasonable explanation could be provided, it would ease the process of introducing a new method of dewatering to industry.

4) The final step would be to discuss ways to introduce the new technology to industry.

CHAPTER 2

LITERATURE SURVEY

A literature survey was conducted with a view to comparing filtration and dewatering, also seen as one-phase and two-phase flow. In this chapter the models of filtration and dewatering, the different types of filtration/dewatering and the equipment used are reviewed. Finally a comprehensive selection of relevant literature on intermitted vacuum application is presented.

2.1 Introduction

Almost all mining processes use water as the carrier fluid for the ore. The water stays in the circuit up to a point where it is removed form the ore, or final processed product. If the water is not removed from the final product, the grade will reduce up to a point where it is no longer a saleable product. The water will also increase handling difficulties. Coal handling is no exception. During washing water is used as the carrier fluid, except during the dense medium separation stages, after which the dense medium is removed from the coal, using water. Finally, the coal has to be dried before it can be sold.

In most mineral processing plants, it is fairly easy to remove most of the water using mechanical equipment like filters and centrifuges. Coal, however, presents difficulties. Coarser lumps can be dewatered to the required moisture levels, but the fine coal (-500μm) poses a problem. The standard moisture levels after dewatering, for fine coal, is in the order of 20-30%, but it may be even higher.

The search for a practical solution to the problem of fine coal dewatering is an ongoing activity. A number of alternative methods, e.g. thermal dewatering, are being evaluated, but usually fail on account of high operating costs.

2.2 Coal and coal plants

2.2.1 The nature of coal

What is coal? How did it form? Coal is a sedimentary rock that contains more than 50% organic material. It was formed more than 200 million years ago by heaping, thickening and hardening of plant residues in different stages of conservation (Snyman, 1996:595-608).

The debris from these plants accumulated under marshy conditions and was transformed to peat, largely by bacterial action. During the conversion process, the plant matter lost moisture, CO_2 was evolved and humic substances were formed (i.e. it turned into compost). The peat bog was ultimately buried under sedimentary deposits and the later stages of the conversion into coal were brought about mainly by the pressure and heat caused by the overlying strata. Roughly speaking, the mass ratio of wood, transformed to coal, is of the order of 20:1. Repetition of the above processes resulted in the formation of different layers or seams, each having its own particular properties (Van der Walt, 1984: 1-22).

Macroscopically, coal consists of different units known as lithotypes. Microscopical studies show that the different lithotypes are made up of one or more homogenic entities of organic materials, known as macerals, as well as small amounts of minerals. These macerals are not crystalline, and their properties and chemical composition are dependent on the rank of the coal. The macerals are divided into three groups, known as vitrinite, exinite and inertinite, each giving a unique property to the coal (Snyman, 1996: 595-608).

2.2.2 Processes for washing coal

With few exceptions modern coal-cleaning processes employ water, as current technology offers no dry beneficiation technique which is effective below 300 μm. Hence, coal preparation plants employ a variety of mechanical dewatering processes (Wakeman, 1984: 53-63).

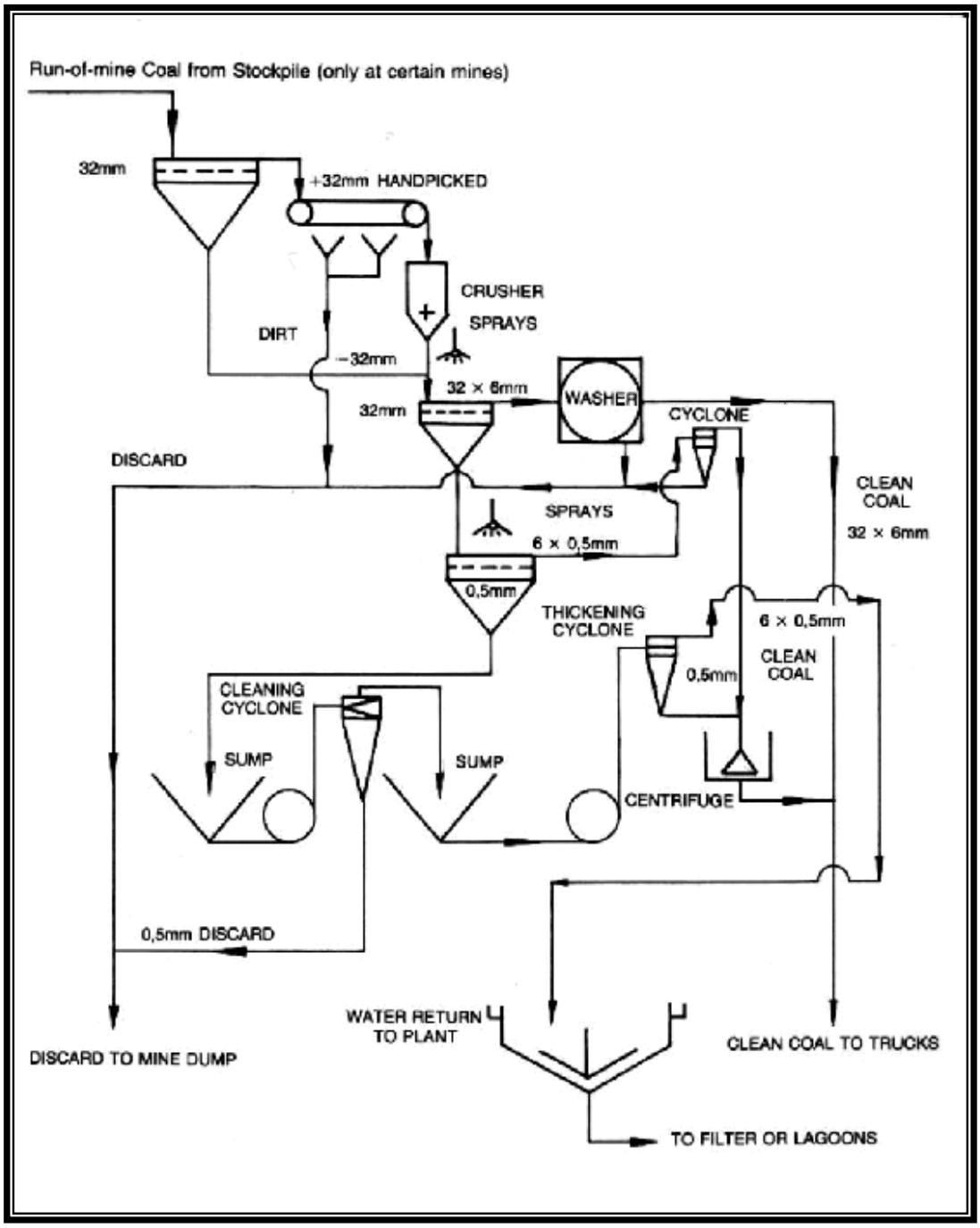

Figure 2.1: A typical coal plant (Horsfall, 1980: 306-340).

Every coal beneficiation plant consisted of the same basic units (building blocks). This led to attempts to design standard units which could be hooked up in new plants, as required. This would have obviated the necessity of designing a complete plant for every new coal beneficiation project. This ideal had to be abandoned because of the special requirements unique to every plant (Horsfall, 1980: 306-340).

Figure 2.1 is a good example of a coal washing plant. As indicated, water forms an integral part of the washing process, resulting in the final step always being the removal of excess water.

2.2.3 Types of water associated with coal

It is useful to collate the terminology in use to describe the forms of water in coal. In considering the water associated with coal in the context of dewatering, it should be noted that essentially only coals of bituminous rank and above are cleaned by wet preparation techniques.

As a first approximation the water in coal could be described on a physical basis as being either interacting (with the coal surface) or non-interacting, depending on whether or not the water in question exhibits the thermodynamic properties of bulk water. However, such a definition presented problems with respect to the actual measurement of the amount of each type of water in a coal/water system (Buckley & Nicol, 1995: 1-12).

For this reason new definitions were developed (Wakeman, 1984: 53-63), which state that water exists within coal in three forms, namely:

1 *Surface water* which lies on the surface of coal particles; this includes moisture held between particles in a coal mass or heap.

2 *Capillary, inherent, or structural water* which is absorbed into the capillary structure of individual coal particles (to avoid confusion of terminology, the term ‘inherent water’ will be used, since much of the so-called surface water

must be regarded as capillary moisture when it exists in the inter-particle pores).

3 *Chemical water*, which is held in chemical combination, usually associated with certain minerals in coal.

Chemically bound moisture was not usually considered to be part of the total moisture content of coal. For this reason mechanical dewatering was only concerned with the first class of moisture, i.e. surface water, which is relatively free to move under imposed pressure gradients. Removing the inherent moisture requires thermal dewatering methods, while chemically bound moisture can only be removed by altering the structure of the coal, e.g. by burning it.

2.2.4 Reasons for dewatering fine coal

Dewatering fine coal is a necessity for obvious reasons. Many studies of the effect of dewatering fine coal have been conducted, highlighting the following reasons why this final step is considered important (Wakeman, 1984: 53-63).

1. Wet coal incurs higher transportation and handling charges. A study done by Tao, Groppo and Parekh (2000: 163-171) showed that even a 1% reduction in the moisture level of the three million tons coal produced annually in the USA, can lead to a saving of US$300,000. Currently in South Africa, this translates to a saving of R2.7 million.
2. Wet coal might freeze and cause handling and utilisation problems in cold weather.
3. Moisture reduces the calorific value of the fuel in combustion processes. It was estimated that a 1% decrease in moisture will give a 1.4% increase in calorific value.
4. Excessive moisture in coke plant charges
   a) increases coking time
   b) makes oven temperature regulation more difficult
   c) contributes to damage of coke oven refractories

d) increases loads on tar and chemical recovery systems

5. Wet refuse requires additional energy for handling.
6. Refuse ponds occupy land, which may be used more profitably.
7. Refuse decantation ponds are unsightly.
8. Pond impoundments can be unstable and constitute a safety hazard.
9. Refuse pond overflows may be of poor clarity, preventing recycling or discharging into streams.
10. Refuse pond sediments may not consolidate enough to make the land usable at a later date.

2.3 Filtration and dewatering

Filtration is the removal of solid particles from a fluid by passing the fluid through a filtering medium, on which the solids build up. Filtration can be done in two basic modes. *Constant pressure filtration* maintains a constant pressure, or vacuum, so that the flow rate falls slowly from a maximum at the start of the cycle. Most continuous filters can be considered to operate on this principle, using vacuum to provide the pressure difference. *Constant rate filtration* requires gradually increasing pressure as the cake builds up and increases the resistance to flow (Kelly & Spottiswood, 1995: 343-366).

Dewatering, on the other hand, is defined as a process whereby water trapped within the void spaces of the filter cake is displaced by the application of desaturating forces to the cake (Venkatadri *et al*, 1994: 71-92). Figure 2.2 shows a schematic of a dewatering process.

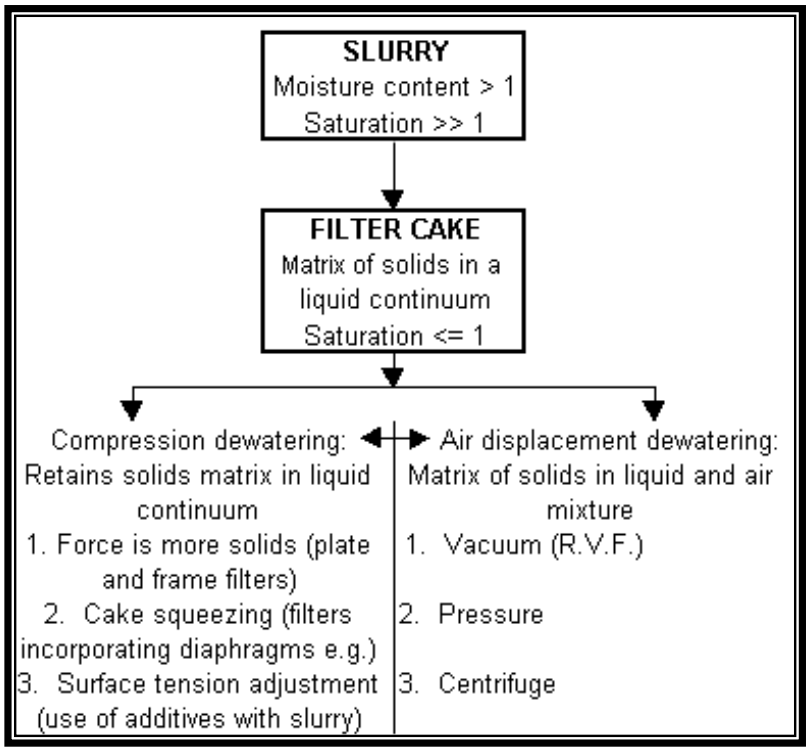

Figure 2.2: A dewatering schematic (taken from Wakeman, 1977: 297-306).

As can be seen from Figure 2.2, filtration constitutes the first part of any dewatering cycle. The formation of the filter cake, likewise, is the first part of the filtration cycle. Therefore, to be able to fully understand dewatering, it is important to start at the beginning, which is the forming of the filter cake, and work all the way up, via filtration to get to dewatering and all the appropriate information regarding dewatering.

2.3.1 Settling of filter cakes

As defined above, during the filtration step there is a build-up of solid particles on the filter medium. As the cake builds up, it acts as a filtration medium in itself, allowing passage only to the liquid phase. The liquid that passes through the cake and the cloth is termed the filtrate.

Once a cake has been built up, a significant quantity of liquid remains associated with the solids, being retained in the interstices of the cake. This residual moisture can be reduced considerably if air under pressure is passed through the cake. Therefore it is important to secure a well-formed filter cake, as shown in Figure 2.3.

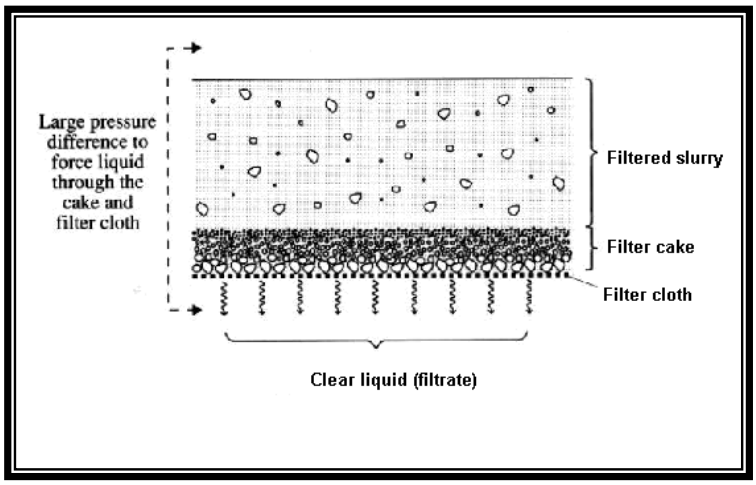

Figure 2.3: A filter cake build-up (Woollacott & Eric, 1994: 125-131).

It is common practice to control the way the cake is formed so that the coarsest particles form a layer closest to the filter cloth, as shown in Figure 2.3. The interstices in this layer will be relatively large so that the rate of filtration is not reduced significantly. As filtration progresses, finer particles penetrate these interstices to some extent and also form further layers on top of the cake. This approach produces a thicker cake than would be obtained if particles of all sizes were allowed to be incorporated in the first layers of the cake (Woollacott & Eric, 1994: 152-131).

This structural build-up usually occurs when a filter cake is allowed to form under the influence of gravitational force only. When the cake is forced to form under a pressure difference, there will be a less uniform size distribution through the cake, which will result in weaker dewatering. Unfortunately, due to the time factor, most cakes in industry are forced to form under differential pressure.

2.3.2 The dewatering cycle

Fine coal dewatering consists of several stages as illustrated in Figure 2.4 (Condie & Veal, 1998: 1-34). The first three diagrams illustrate the forming of the filter cake, involving single phase flow of fluid through the cake. In the last three diagrams, the dewatering process, which involves two phase flow, is illustrated.

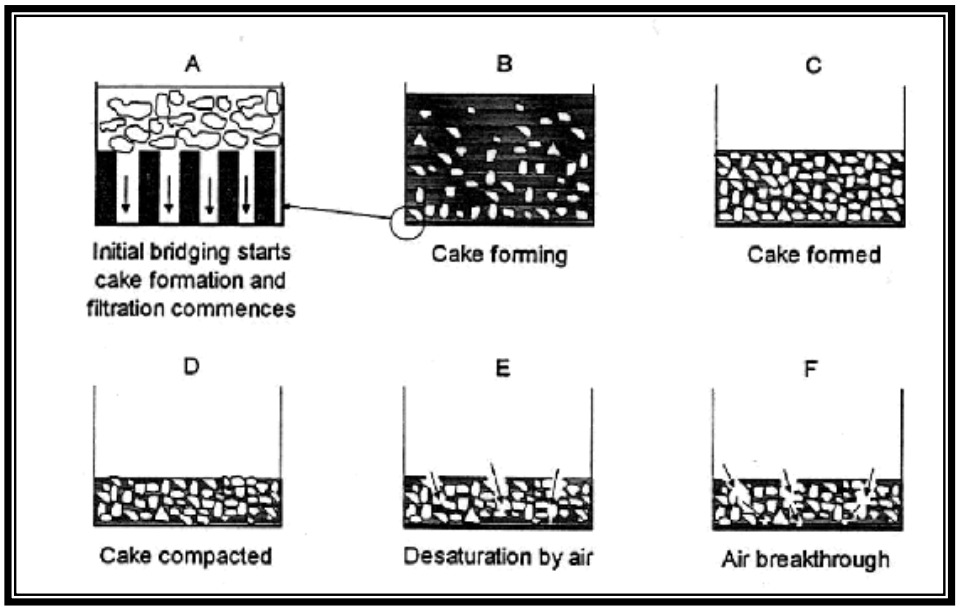

Figure 2.4: Stages of dewatering (Condie & Veal, 1998: 1-34).

Diagram A shows the initial bridging of particles across the filter medium as the first few layers of the filter cake start to form. This is followed by the completion of the filter cake and filtration, characterised by a continuously increasing cake thickness and single phase flow through the forming cake, as illustrated by Diagrams B and C. This stage can be very efficiently modelled as a simplified plug-flow model.

The flow of the wetting fluid through the bed during cake formation is classically described by Darcy's law

$$\frac{dv}{dt} = \frac{KA\Delta P}{\eta L} \qquad (2.1)$$

where dv/dt is the rate of filtrate flow while ΔP is the pressure difference across the filter cake.

The continuous flow of water through the cake leads to some form of cake compression (Diagram D, Figure 2.4), *i.e.* water expression. This aspect is, however, not very important when working with –500 μm coal, since the cakes formed are not appreciably compressible under vacuum (Condie & Veal, 1998: 1-34).

Diagram E (Figure 2.4) depicts the start of desaturation of the filter cake by two phase flow of filtrate and air, through the filter cake, during which the largest pores are first being emptied of water. The smaller pores, on the other hand, remain either partially or totally saturated. This will continue to a point where air breakthrough occurs (Diagram F, Figure 2.4), which is characterised by the emptying of filtrate from the largest pores, and the flowing of air through them. The smaller pores still contain filtrate, some of which is being removed slowly (Condie & Veal, 1998: 1-34).

2.3.3 Capillary Pressure (Dewatering) curves

Capillary pressure curves are obtained by increasing the pressure difference over the cake in increments until no further liquid flows from the cake. Figure 2.5 shows a typical curve. No dewatering takes place until the applied pressure P reaches a threshold value P_T, which is a measure of the largest pore in the filter cake. The value of P_T is often ill-defined and it is usual to define a modified threshold pressure P_b as shown in Figure 2.5. As the pressure increases, liquid is displaced from increasingly smaller pores until further increase in pressure does not result in further reduction in saturation. All the capillary liquid has then been removed and the remaining liquid defines the irreducible saturation point, S_∞ (Carleton & Mackay, 1988: 1-34).

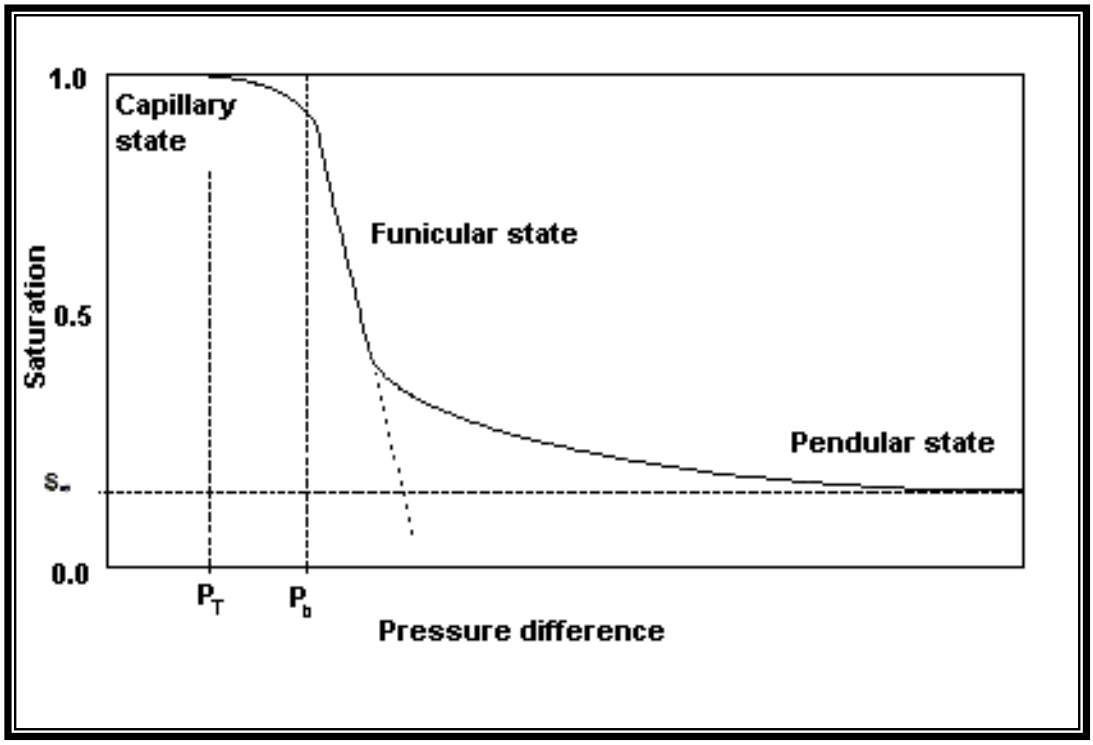

Figure 2.5: Capillary pressure curve.

As shown in Figure 2.5, capillary pressure curves display three different dewatering states, namely the capillary state, the funicular state and the pendular state.

Capillary state.

At zero or low pressure, and provided the cake is thin, if the interparticulate voids remain saturated, the cake is said to be in the capillary state. An opposing pressure, referred to as the capillary pressure, generally prevents entry of air.

The concept of capillary pressure is worthy of a clarification before proceeding further. Liquid displacement is opposed by the relative magnitude of the forces of molecular attraction between the phases present at the three phase contact. Surface tension forces are the familiar manifestation of these attractive interactions. The resultant action of all these forces is such, that at any given relative saturation, a certain pressure differential in the displacing phase versus the displaced phase will have to be maintained to create equilibrium (Buckley & Nicol, 1995: 1-12).

Funicular state

As displacement proceeds, a funicular state is reached in which a continuous network of water exists in equilibrium with air interdispersed throughout the porous assembly. Since the radius of a pore is greater than the radius of a throat, water will flow freely once the threshold pressure is exceeded. The equilibrium moisture content at any given pressure is then determined by the Laplace pressure at the surface of the network of liquid "lenses" formed at the points of contact between neighbouring particles.

The threshold pressure, for the identical packing of monodisperse spheres, is inversely proportional to the sphere radius, therefore the moisture retained by such a model system, while in the funicular state, will also be inversely proportional to the sphere radius for any given applied pressure. The steep slope of the curve reflects the assumed monodispersed nature of particles (Buckley & Nicol, 1995: 1-12).

Pendular state

This state corresponds to the formation of discrete liquid lenses at particle contacts, and represents the limit of the pressure/moisture curve and therefore the limit of dewatering by filtration (Buckley & Nicol, 1995: 1-12). If it is necessary to remove any more liquid from the cake, thermal dewatering must be used.

2.3.4 Models describing the dewatering of fine coal

Various models describing the dewatering of fine coal have been developed. The first of these was as early as 1933 by Ruth, and was an empirical model (Ruth, 1933: 708). Almost all models that followed were semi-empirical, using experimental work to calculate the values of certain parameters.

One of the most common ways to address this issue, although also semi-empirical, was to study the two-phase flow of a fluid through a filter cake. For this, the Reynolds number was adjusted to describe the saturation point of the cake, as well as the capacity of either the vacuum- or pressure pump. A good example of this is a model that was developed by Brownell and Katz (1947: 537-548).

Theoretical approaches have been tried, but to no avail. One such an example is a model developed by Walker and Svarovsky (1994: 57-65). This model concentrated on describing the continuous thickening of the filter cake and its characteristics. Another variable that was studied was the decreasing flow rate of the filtrate in relation to the thickening of the filter cake. Unfortunately this model, to date, is only suited for use on spherical particles (Condie & Veal, 1998: 1-34).

One model stood out as being useful in describing the process of dewatering fine coal. This was a model, developed by Wakeman in the late 1970s (Wakeman, 1979: 379-393). Condie & Veal (1998: 1-34) found that this model gave a good representation of the actual dewatering process, especially when working with fine coal. The reasons are as follows:

- The model seemed easy to use
- In comparison with other models, this model gave very good results for the dewatering of fine sand
- The model was used with distinction in previous projects (Condie & Veal, 1998: 1-34).

For these reasons it was considered to apply Wakeman model in this project.

2.4 A description of Wakeman's model

Wakeman's model can be used to calculate the following:

- The saturation in the filter cake, at equilibrium, at any given vacuum
- The dewatering profile, relative to time
- The airflow needed to dewater the cake

The parameters used for dewatering during equilibrium conditions, namely breakthrough pressure, equilibrium saturation and pore size distribution index, can then be used to develop equations to predict the kinetics of moisture reduction and air flow (Condie & Veal, 1998: 1-34).

2.4.1 Wakeman's model for the prediction of dewatering kinetics

During the development of his dewatering models, Wakeman looked at both the flow of air and water through the filter cake. In doing so, he rewrote Darcy's law (Eq. 2.1) in the following form:

$$V_i = \frac{-KK_{ri}}{\eta_i}\frac{\partial P_i}{\partial x} \tag{2.2}$$

where V is the volumetric flux density relative to the solids and $\partial p/\partial x$ the fluid pressure gradient while the subscript *i* can be changed to a or L, depending on whether it refers to air or water. The product KK_r is the effective permeability of the filter cake. It is thus an indication of the filter cake's ability to let fluid through at any saturation point.

For fluid flow to be continuous, any solution of Darcy's law must also obey the following material balances:

$$\varepsilon\frac{\partial S_L}{\partial t} = -\frac{\partial \upsilon_L}{\partial x} \tag{2.3}$$

$$\varepsilon\frac{\partial (S_a \rho_a)}{\partial t} = -\frac{\partial (\upsilon_a \rho_a)}{\partial x} \tag{2.4}$$

where the porosity, ε, was assumed to be independent of time and the location in the cake. The residual fluid was assumed to be incompressible.

The fluid saturations and pressures were related according to subsidiary equations:

$$S_L + S_a = 1 \tag{2.5}$$

$$P_a - P_L = P_c \tag{2.6}$$

with P_c the capillary pressure.

Equations 2.2 to 2.4 may be solved, subject to the subsidiary Equations 2.5 and 2.6. In a general laboratory experiment, it is likely that the pressure at the cake/cloth interface measured in the air phase will rise during vacuum dewatering, as the liquid saturation in the cake decreases. It will happen, despite the ability to keep the applied vacuum constant at the required needs. This is commonly known as a low capacity system. Boundary conditions for such a system were derived by Wakeman, and is given in Equations 2.7 and 2.8 (Wakeman, 1976: 193-206).

$$P_L|_{x=L} = f_1(S_L) \qquad 0 < t < t_b \qquad x = L \tag{2.7}$$

$$P_a|_{x=L} = f_2(S_L) \qquad t > t_b \qquad x = L \tag{2.8}$$

where t_b was the breakthrough time at the cake cloth interface.

Both $f_1(S_L)$ and $f_2(S_L)$ were unknown functions of saturation. Wakeman showed, through experimental work, that $f_1(S_L)$ was almost independent of saturation, the reason being a negligible loss of vacuum until air has penetrated the entire depth of the cake. $f_2(S_L)$ was determined experimentally, and was related to the vacuum level by a cubic equation for liquid saturation as follows:

$$\frac{P_a(L,t) - P_a(L,t \to \infty)}{P_a(L,0) - P_a(L,t \to \infty)} = a_1 S_R + a_2 S_R^2 + a_3 S_R^3 \tag{2.9}$$

where $P_a(L,t)$ is the air pressure at the cake/cloth interface at time t, $P_a(L,0)$ is the initial vacuum level, and a_1, a_2 and a_3 are constants evaluated from a least squares fit of the pressure term on the left hand side of Equation 2.9 to the average reduced saturation of the cake, S_R (averaged over the distance $0 \le x \le L$). S_R was defined by:

$$S_R = \frac{S_L - S_{L\infty}}{1 - S_{L\infty}} \tag{2.10}$$

where S_L, $S_{L\infty}$ and $P_a(L,t)$ were all determined experimentally (Wakeman, 1977: 297-306).

The boundary conditions for the air inflow simply state that there is no flow of residual filtrate into the cake, *i.e.*:

$$t \ge 0 \qquad x = 0 \qquad v_L = 0 \tag{2.11}$$

The capillary pressure curves are then determined by substituting the equilibrium saturation point S_e (this is the saturation of the filter cake at time t_∞ for given dewatering situations) in Equation 2.10, and is given in Equation 2.12.

$$S_{RE} = \frac{S_e - S_{L\infty}}{1 - S_{L\infty}} = \left(\frac{\Delta P}{P_b}\right)^{\lambda} \tag{2.12}$$

where λ is the pore size distribution index (Condie & Veal, 1998: 1-34).

This Equation is only valid for the region where S_R has a value of less than one. A graph of $-lnS_R$ vs. $ln(\Delta P/P_b)$ gives a straight line, with a slope equal to the pore size distribution index (λ). Wakeman assigned a value of 5 to λ. This was acceptable, since most of his work was done on sand and glass beads (Condie & Veal, 1998: 1-34). When working with fine coal, a value of 5 for λ is unacceptable, and therefore, a new value will have to be determined.

Another way of determining the breakthrough pressure was published by Carleton and Mackay (1988: 187-191):

$$P_b = \frac{\omega\gamma\cos\beta(1-\varepsilon)}{d_k\varepsilon} \qquad (2.13)$$

2.4.2 Relative permeability

Before Wakeman could derive an equation for relative permeability, there were two special features of relative permeability that he had to study. Firstly, the relative permeabilities fall to zero well before the saturation of the respective phase change reaches zero, and secondly, for saturations less than 100%, the sum of the two relative permeabilities is less than one. It is important for any model to correctly interpret these features. In the past many dewatering models were wrong in their interpretation of the relative permeability of a filter cake, including the widely used "bundle of tubes" model (Wakeman, 1977: 297-306).

Wakeman found the pores in a filter cake not to be of uniform shape, and he established that no single pore passed through the cake. Pores consisted of many branches, interconnections and shape irregularities. By using a simple "cutting and rejoining" model, he found an expression for relative permeability, given in Equations 2.14 and 2.15 (Wakeman, 1977: 297-306).

$$K_{rL} = S_R^2 \frac{\int_0^{S_R} \frac{dS_R}{[P_c(S_R)]^2}}{\int_0^{1} \frac{dS_R}{[P_c(S_R)]^2}} \qquad (2.14)$$

$$K_{ra} = (1 - S_R)^2 \frac{\int_{S_R}^{1} \frac{dS_R}{[P_c(S_R)]^2}}{\int_{0}^{1} \frac{dS_R}{[P_c(S_R)]^2}} \tag{2.15}$$

He then derived functional relationships between the relative permeability and the reduced saturation, which is given in Equations 2.16 and 2.17.

$$K_{rL} = S_R^{(2+3\lambda)/\lambda} \tag{2.16}$$

$$K_{ra} = (1 - S_R)^2 (1 - S_R^{(2+\lambda)/\lambda}) \tag{2.17}$$

2.4.3 Dewatering equations in dimensionless form

To facilitate the solving of his model, Wakeman derived a few dimensionless equations (Equations 2.18 – 2.22), using dimensionless pressure, flow rates and time.

$$P_L^* = \frac{P_L}{P_b} \tag{2.18}$$

$$P_a^* = \frac{P_a}{P_b} \tag{2.19}$$

$$\upsilon_L^* = \frac{\upsilon_L \mu_L L}{K P_b} \tag{2.20}$$

$$\upsilon_a^* = \frac{\upsilon_a \mu_a L}{K P_b} \tag{2.21}$$

$$\theta = \frac{K P_b t}{\mu_L L^2 \varepsilon (1 - S_L)} \tag{2.22}$$

Using these dimensionless equations, Equations 2.2–2.4 and 2.6 reduced to the following:

$$V_L^* = -S_R^{(2+3\lambda)/\lambda} \frac{\partial P_L^*}{\partial (x/L)} \tag{2.23}$$

$$V_a^* = -(1 - S_R)^2 (1 - S_R^{(2+\lambda)/\lambda}) \frac{\partial P_a^*}{\partial (x/L)} \tag{2.24}$$

$$\frac{\partial S_R}{\partial \theta} = -\frac{\partial V_L^*}{\partial (x/L)} \tag{2.25}$$

$$\frac{\partial\{\rho_a(1-S_R)\}}{\partial\theta} = -\frac{\eta_L\partial(\rho_a V_a^*)}{\eta_a\partial(x/L)} \quad (2.26)$$

where ρ is the density of the fluid. The discontinuity at the air and filtrate residue interface in the cake is given by:

$$\rho_a^* - \rho_L^* = S_R^{-1/\lambda} \quad (2.27)$$

Wakeman solved Equations 2.8-2.12 by dividing the filter cake into smaller increments, each one with its own initial pressure and saturation point. He then calculated the progression of the frontmost end of the air as it moved through each of the increments. An assumption was made that as the air moved on, the remaining filtrate will move through a part of an increment with thickness $\Delta(x/L)$ to form a new increment. By repeating this, the filtrate will move to the bottom of the filter cake, and will eventually be disposed of (Baluais, Dodds & Tondeur, 1985: 436-446). The method of solution is outlined in Appendix D.

2.4.4 Boundary conditions and assumptions

The use of Wakeman's model requires many assumptions as well as certain boundary conditions. Most of these assumptions are valid, while the influence of others is limited.

Compressibility of the filter cake

The first assumption to be made is that coal filter cakes are incompressible. This simply means that the filter cake does not change its structure during the dewatering process. Unless forced, the permeability also does not change. Kukard (2001), using South African coal, showed this assumption to be valid. Condie and Veal (1998: 1-34) also showed that a coal filter cake is compressible, but to such a limited extent that it has relatively little influence on the use of the model. In most cases cake compressibility is evident when a pressure difference of more than 1 bar is present over the filter cake. In vacuum filtration, this pressure difference will never be reached, thus making the assumption valid.

Medium resistance

To incorporate the medium resistance into the equation, it needs to be measured experimentally, converted to relative cake thickness and used as an extra cake resistance in series.

Cake uniformity

For cakes thicker than 10mm, it was assumed that the filter cake which formed had a uniform thickness and that the porosity of the cake was independent of the thickness of the cake. For this reason it is important to make sure that the filter cake is always of a uniform thickness, of more than 10mm.

Boundary conditions

At the start, it can be taken for granted that the coal is 100% saturated, meaning that S = 1. Therefore, because at time t = 0 no further water will flow into the system, it can be assumed that $K_{rL} = 0$ and $S_L = S_{L\infty}$. The saturation gradient just inside the air inflow face will be very steep. After air breakthrough the driving force exists as a continuous gas pathway through the voids, and P_a is a constant throughout the cake at the initial value of the fluid pressure at the outflow face. This assumption was shown to be correct, since it has very little influence on the system (Condie & Veal, 1998: 1-34).

The mechanism of moisture removal

All the moisture in the cake is assumed to be removed by displacement air flowing into the cake from the atmosphere. It is also assumed that no evaporation of water occurs to the atmosphere during the dewatering cycle.

This assumption was validated by studying the time it takes to dewater a coal filter cake. It was assumed that the time does not take longer than 120s, which will mean that there simply is not enough time for the water to evaporate (Condie & Veal, 1998: 1-34).

The contact angle term

The model of Wakeman does not contain any term for the water/particle contact angle. Wakeman himself (1979: 395-405) as well as Carleton and Mackay (1988: 187-191) verified this, using hydrophilic materials such as fine sands for which the contact angle will be zero. The validity of this assumption for coal and therefore its influence, is unknown.

Capillary pressure curve parameters

Wakeman gave values of 4.6 and 5 for the constant in Equation 2.3 to calculate the breakthrough pressure and the pore size distribution index respectively. These values are only applicable to the materials he used, and new values have to be determined when working with coal.

2.5 Filtration types and equipment

It is interesting to note where the above-mentioned theory finds application in industry. For this reason a brief summary of industrial filter types and filter equipment will be given.

In industry, two common types of filtration are found, namely vacuum filtration and pressure filtration. A third dewatering technique, centrifugation, is also employed, but its kinetics differs from that of the other two. Where the driving force in filtration is a pressure difference across the filter cake, the driving force for centrifugation is centrifugal forces acting on the formed cake.

2.5.1 Vacuum filtration

Vacuum filtration is the most commonly found form of filtration and dewatering in industry today. Some of the reasons for this are that it is the most economically operated system of all the filtration types. The fact that it can be operated in a continuous manner also weighs heavily in its favour. A third factor that makes vacuum filtration popular is that it is operated at approximately atmospheric pressure, thus making it very safe (Woollacott & Eric, 1994: 125-131).

The limitation imposed by a maximum of 1 atmosphere vacuum is also the biggest drawback of vacuum filtration. It is generally accepted that the greater the pressure difference across the filter cake, the more effective the dewatering.

Vacuum filtration equipment can be divided into three classes. Firstly there are the drum filters, followed by disc filters and finally horizontal filters, of which the belt filter is the best example. The only difference between these three is the way the filter cake forms and the way it is discarded. Figure 2.6 illustrates the three types of filters.

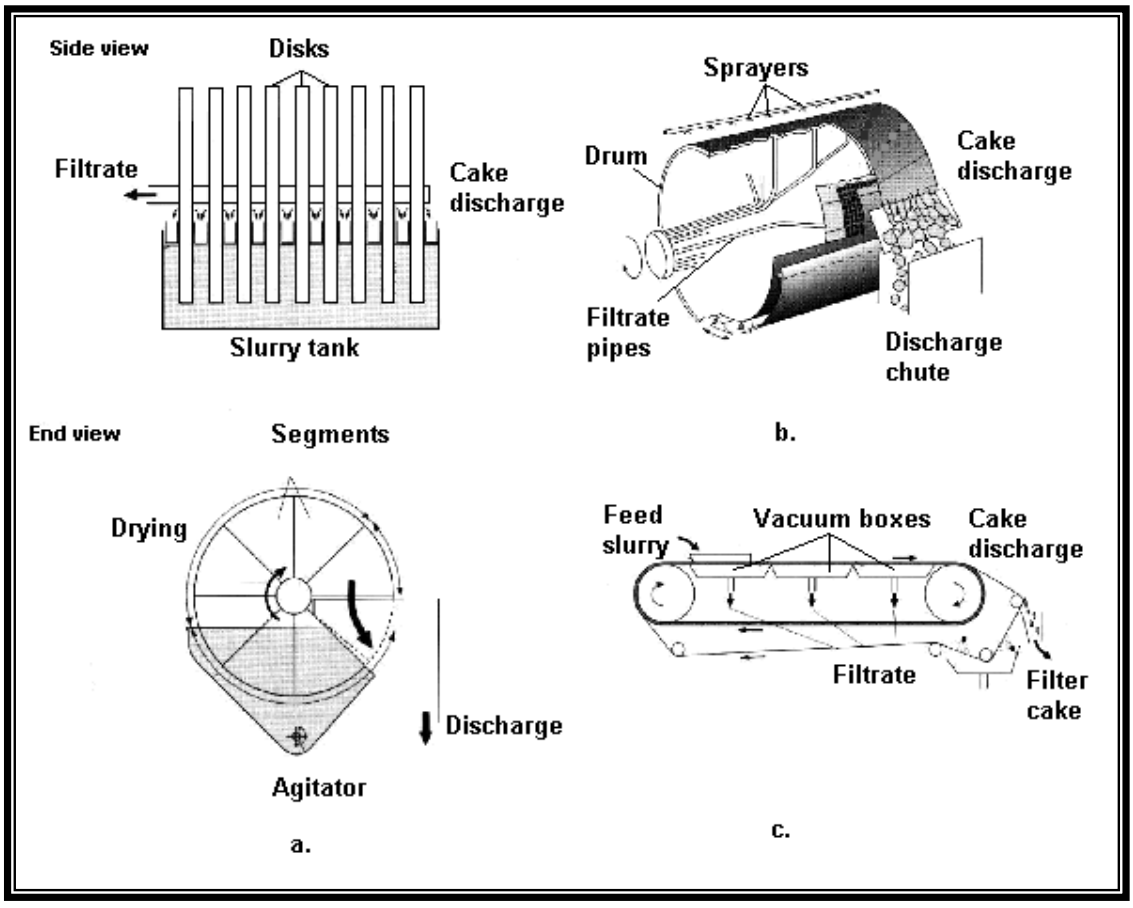

Figure 2.6: Vacuum filtration equipment: a. Disc filter. b. Drum filter. c. Belt filter (Woollacott & Eric, 1994: 125-131).

2.5.2 Pressure filters

Pressure filters have the capability of creating a high pressure difference across a filter cake, thus theoretically giving a drier filter product. This works well in batch processes, and applied pressures of up to 4 atmospheres are not uncommon.

Unfortunately these high pressures cause many problems for the filters by creating an unstable environment and causing safety hazards. Another big problem encountered with pressure filters is their inability to operate continuously. Several pieces of equipment have been designed with this goal in mind, but none were successful. The most promising to date is the filter press (Figure 2.7) which operates in a semi-batch mode (Woollacott & Eric, 1994: 125-131).

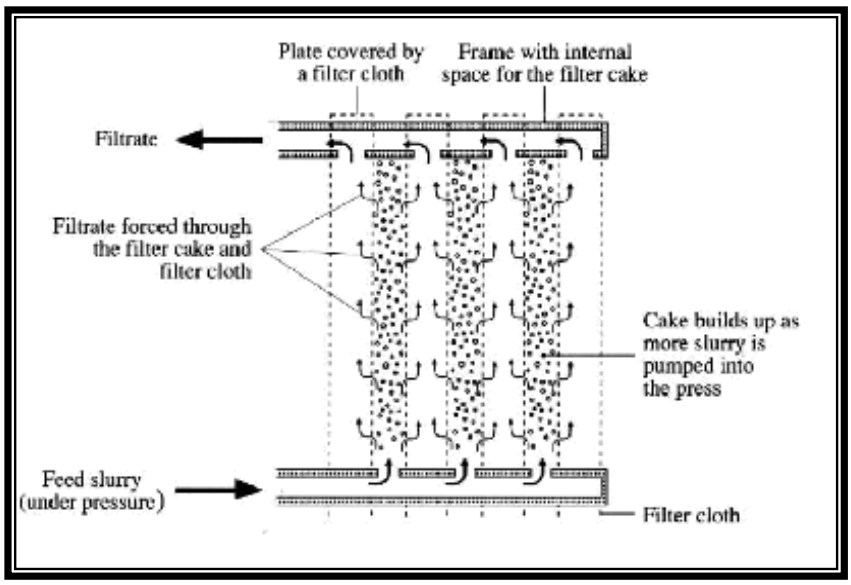

Figure 2.7: The filter press (Woollacott & Eric, 1994: 125-131).

2.5.3 Centrifuges

Centrifuges were initially designed with sedimentation in mind, and were later used as dewatering equipment. Centrifuges have the quality of giving a discard with a much lower percentage moisture than vacuum filters and pressure filters. The reason for this is the high centrifugal forces that can be created when the centrifuge is spinning at speeds of up to 6000 r/min.

Although the relative maintenance costs for centrifuges are low, the high rotational speed of the centrifuge does constitute considerable wear and tear on the bearings. They require more frequent replacement than in other dewatering equipment (Woollacott & Eric, 1994: 125-131). Another major disadvantage of centrifuges is their tendency to lose solids, which is estimated to be about 5% (Rong & Hitchins, 1994: 86). Figure 2.7 is a schematic drawing of a solid-bowl centrifuge.

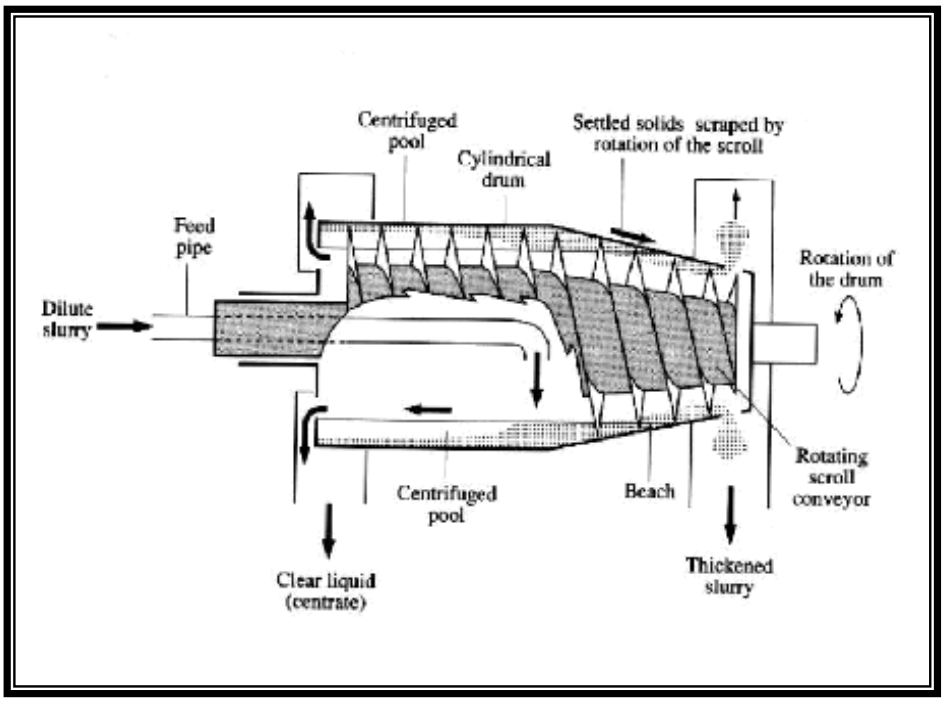

Figure 2.7: A solid-bowl centrifuge (Woollacott & Eric, 1994: 125-131).

2.6 A new method for dewatering fine coal

In 2000, while determining capillary pressure curves, and in particular the pore size distribution index for South Africa's Waterberg coal, it was found that a release of vacuum to atmospheric level at regular intervals during a capillary pressure curve determination, gave a final cake with much lower moisture content than before (Le Roux, 2000). This study also showed that vacuum release had a positive effect on the kinetics of dewatering.

Generally, the dewatering curves moved to the left, indicating the elimination of the capillary state, with the process starting at the funicular state. This implied the achievement of several advantageous features: firstly, a higher rate of dewatering, secondly, a much lower breakthrough pressure, and finally a much drier product.

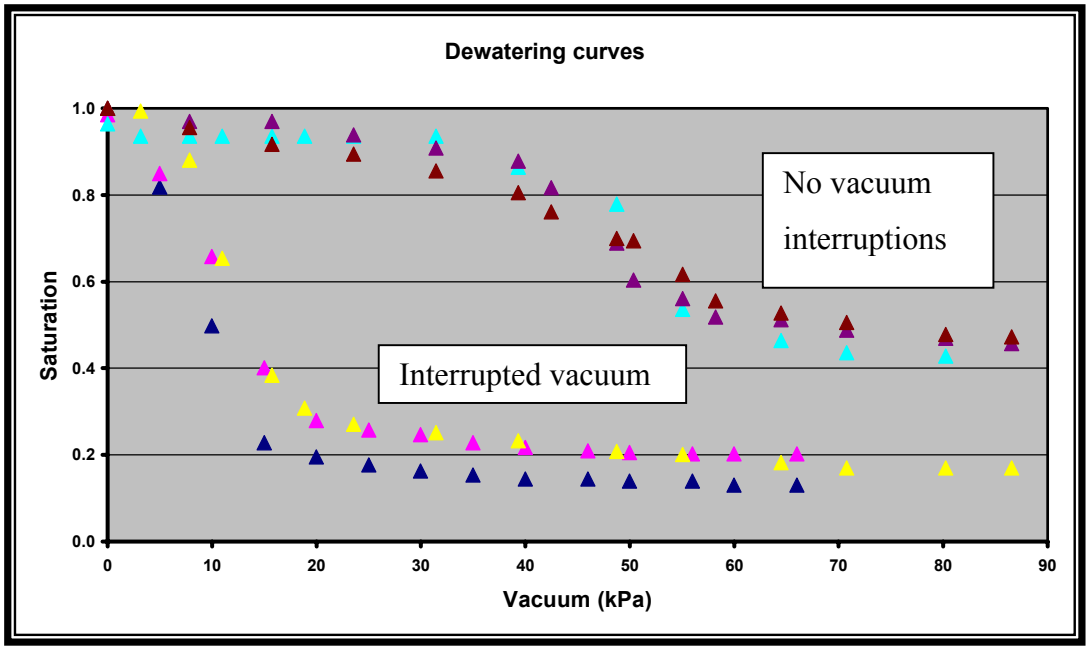

Figure 2.8: Capillary curves for release in vacuum (Le Roux, 2000).

A subsequent literature search yielded only one reference to this phenomenon, the results of which are shown in Figure 2.9 (Carleton & Mackay, 1988: 187-191). This work refers to results obtained with sand and glass beads, but the same effect was found. It clearly shows the shifting of the curves to the left, eliminating the capillary state. It also shows a much lower breakthrough pressure and a better dewatering rate.

What is interesting to note, is that these tests were done using low pressure as driving force, and not vacuum. Although the reason for this is not explicitly given, it can be assumed that the airflow through the cake is the main contributor. In a nutshell: it means that a high airflow was required, which was obtained at low pressure.

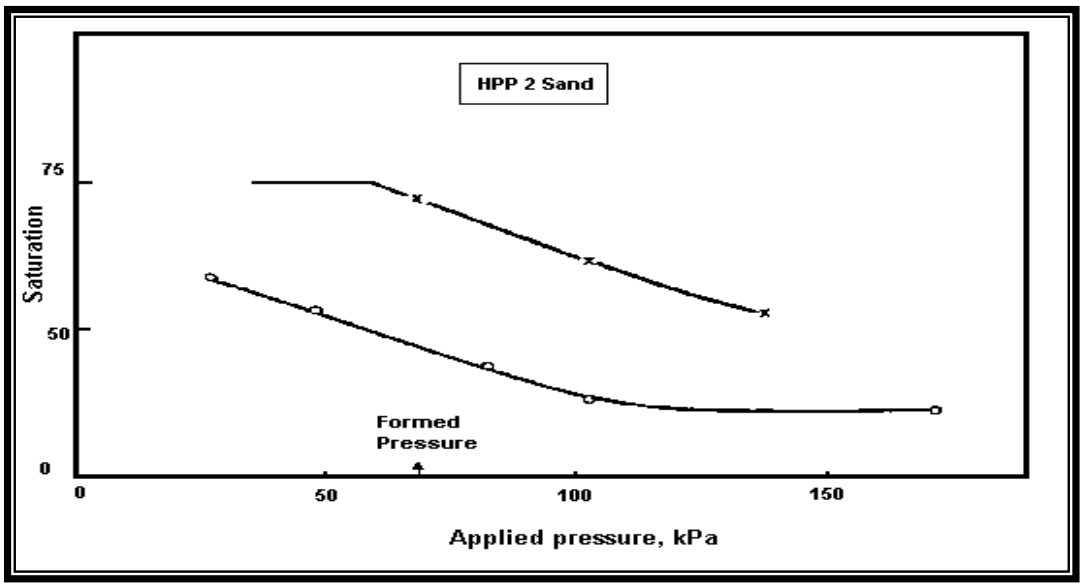

Figure 2.9: Capillary curves by Carleton and Mackay (1988: 187-191).

The authors did not advance an explanation for the phenomenon and they did not pursue the matter further.

CHAPTER 3

EXPERIMENTAL

The correct experimental setup is vital for any research project. Careful consideration must be given to the building of the equipment, the coal that will be used and the methodology, including experimental planning. This chapter is devoted to these aspects of the project, and will also describe the relevant experimental procedures.

3.1 Introduction

The correct experimental setup is vital for any research project. In trying to achieve industrial standards, it was decided to emulate existing industrial belt filters on a laboratory scale. Ultimately, it would also ease the process of upgrading to industrial scale application, in line with the scope of the project (see Section 1.3). The New Vaal Collieries plant was chosen as reference facility for this purpose.

To be able to achieve this, aspects of the New Vaal Collieries' filters were studied, including:

- The filter cloth
- The retention time of coal on the filter
- The thickness of the coal filter cake, and
- The type of coal that was used

These features were considered while designing the equipment and planning the experimental procedure.

3.2 Equipment

3.2.1 The filter setup

A bench scale filter was constructed of glassware. It was batch-operated, with interchangeable heads for using a filter cloth as well as membranes as filter media. Figure 3.1 is a photograph of the set-up while Figure 3.2 is a schematic drawing of the filter system.

Figure 3.1: The filter set-up.

The system consisted of a glass bell which could be evacuated. The interchangeable filter heads fitted onto the top of the bell. A glass beaker, situated inside the bell, was used to collect the filtrate. It was placed on a loadcell to increase the accuracy of the filtrate mass measurements.

Initially a control valve was fitted to the system in an attempt to increase the accuracy of the applied vacuum step changes. Pre-testing showed the valve to lack in response time. It was therefore replaced with a three-way valve for rapid changes, and a needle valve for finer adjustments. The vacuum was therefore controlled manually. Data logging was done by computer.

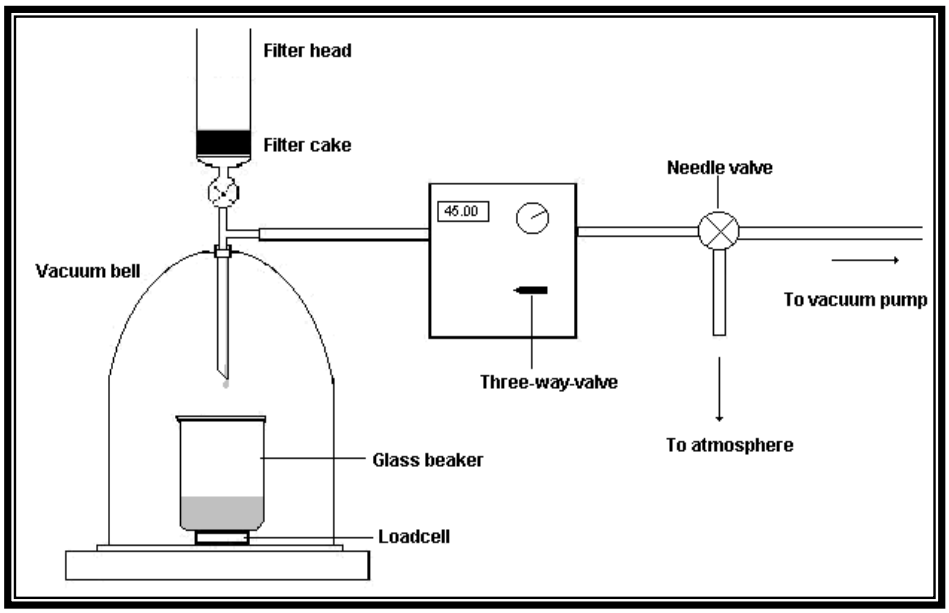

Figure 3.2: A schematic drawing of the filter system.

3.2.2 The funnel

Figure 3.3 shows the funnel that was used. It was a normal borosilicate glass funnel, based on the Buchner design, with the top of the funnel extended to accommodate the dilute feed slurry. Because the funnel was made of borosilica, the extension was glued onto the funnel, instead of being melted.

The dimensions of the funnel were as follow:

- Diameter = 67 mm.
- Height = 280 mm.

Figure 3.3: The funnel.

3.2.3 The filter cloth

The filter cloth, obtained from New Vaal Collieries, was a Devtex 356 cloth (shown in Figure 3.4) with the specifications given in Table 3.1. It is the same filter cloth currently in use on both the belt filters operating at New Vaal Collieries.

Table 3.1: Filter cloth specifications.

Variable	Description
Quality number	Devtex 356
Material	100% Polyester
Threads	24 cm^{-1}
Weight	828 $g.m^{-2}$
Air permeability	990 ± 10% $l.dm^{-2}.min^{-1}$
Thickness	1151μm
Tensile strength	1330 ± 10% $N.cm^{-1}$

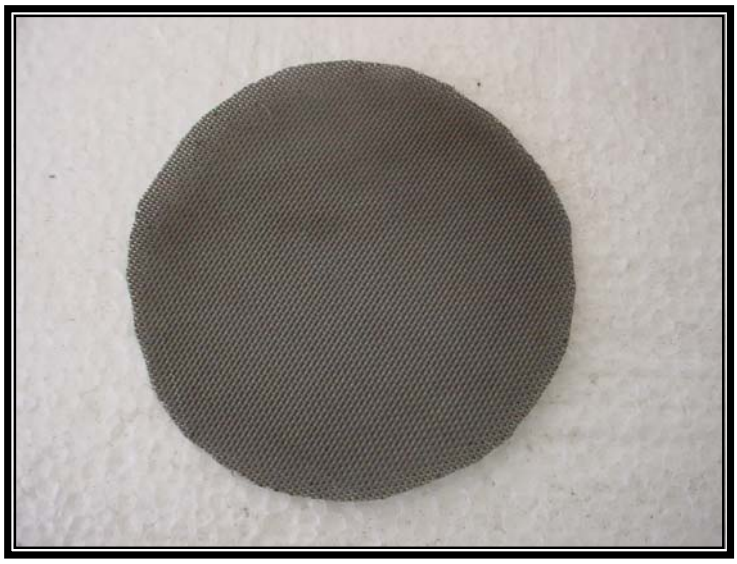

Figure 3.4: The filter cloth.

3.3 Material used

Thickener underflow material from New Vaal Collieries was used for the experimental work. The thickener underflow is pumped to the belt filters as feed, and therefore was ideal for use in the laboratory.

After obtaining the sample, it had to be prepared for use, which included drying, sieving, and doing a proximate analysis on the coal.

3.3.1 Preparation of the coal

About 25 litres of thickener underflow was sampled. Preparation on the coal started by drying the sampled slurry. First it was filtered through large pressure filters to remove all the excess water. Two pieces of filter paper were used as filter medium. This was done to secure a minimum loss of solids during the drying process. Afterwards the coal was spread open and air dried for a few days, before the remaining moisture was driven off in a drying oven at 60°C. Care was taken not to set the oven temperature much higher than 60°C, since it could change the structure of the coal, or ignite/remove volatile constituents.

Using a laboratory splitter, the dry coal was then split into two samples: one for immediate use, and the other to act as control sample. As accuracy of the splitting method was unknown, it was decided to use the same splitting method to prepare samples for particle size analysis. Thus any differences between samples would be revealed.

3.3.2 Particle size analysis

The working sample was split into five different samples of 200g each. Each sample's particle size was determined separately, using a √2 series, starting at 75μm. 75μm is commonly assumed to be the smallest particle size where dry sieving is accurate, while 600μm was chosen as upper limit, for practical reasons.

3.3.3 Proximate analysis

Due to the diversity of coal, it was important to try and characterise the coal as well as possible. Several international standards have been developed to assist in creating a common database for researchers to refer to when working with coal (see Table 3.2). This is called the proximate (prox) analysis. These tests were done in the laboratory of Potchefstroom University.

Table 3.2: Proximate analysis standards.

Test	Standard
% Moisture	SABS 924
% Ash	ISO 1171
% Volatile matter	ISO 562
% Fixed carbon	-
Calorific value	Bomb calorimeter.

3.4 Experimental planning

With any project, it is important to plan the experimental work very carefully, keeping in mind the objective of the proposed project. It is, however, also important to keep plans flexible in order to facilitate unforseen adaptations that may be required.

As was discussed in Section 3.1, the experimental set-up was designed in such a manner that it emulated the existing belt filters at New Vaal Collieries. It was therefore important to plan the experiments accordingly. After a study of the New Vaal Collieries filters, the following strategies, called the "plant constants", were identified:

- The first important issue was the retention time of the coal on the filter. With the filters running at a constant speed, this was not difficult to determine. From the point of 100% saturation it took a coal particle approximately 5 min (300s) to reach the end of the belt and be discarded. Thus the length of each run was determined as 300s.
- Secondly was the thickness of the filter cake. This was found to be between 10 and 20mm, with an average of 15mm. In the lab this translated to 40g of dry coal per experiment.
- The vacuum applied to the filter was 45 kPa; the same as at New Vaal Collieries.
- The same filter cloth was used, as on the plant.

With the plant constants known, the rest of the planning consisted of the inclution of the following additional features.

- The whole project was based on the hypothesis that an interruption in the applied vacuum during a dewatering cycle would result in a drier final product. The questions to be addressed were the following:
  - How long should the duration of this interruption be (break duration time)?
  - At what point in the dewatering cycle should this interruption occur (initial break time)?
  - How many interruptions in applied vacuum should there be during a single dewatering cycle?

It was decided to use three different break duration times, namely 15s, 30s and 60s. Using a 30s break duration time will only decrease by 10% the time where the filter cake is subjected to vacuum. 15s and 60s were chosen on the basis of cutting the 30s break duration time in half, or doubling it. The initial break time was chosen to start at 15s, and every 15s thereafter, for the subsequent tests. The number of interruptions would depend on the results of the single interruption tests, varying the break duration times and initial break times.

To try and increase productivity, it was decided to vary the initial break time for the whole dewatering cycle only for the 30s break duration tests. Afterwards an optimum range for the initial break time was calculated. Therefore for the 15s- and 60s break duration tests, the initial break time was varied inside this optimum range.

- For statistical reasons, each of the tests was triplicated, to obtain an average of three tests. This increased the accuracy of the tests.
- The experiments for repeating the interruption in vacuum were planned after the results of the first experiments were available. This included the break duration time, the initial break time and the amount of interruptions in a cycle.

- Finally, from the control sample, the -100μm and -200μm coal were sieved and used only at the optimum point, to show the influence of the ultra fine particles on the dewatering of coal.

The full experimental schedule is shown in Appendix A.

3.5 Experimental procedure

The experimental procedure is given in bullet form below:

- Weigh 40g of coal from the working sample and put it in a beaker.

- Add a known amount of water to the weighed sample.
- Prepare the filter and make sure the vacuum setting is at 45 kPa. Check that the filter cloth is cleaned, sealed and also make sure the valve to the funnel is closed, so that no vacuum will reach the funnel. The bell must be under vacuum though.
- Stir the slurry rapidly for about one minute, and pour it into the funnel.
- As soon is all the slurry is poured into the funnel, the valve must be opened to assure that the filter cake will form under hindered conditions. The beaker inside the bell will start to fill up with filtrate.
- As soon as the 100% saturation mark is reached, set the computer to start with the automatic data logging. The 100% saturation mark is the visually defined point when the meniscus of the water is no more than a millimetre above the top of the filter cake.
- Break the vacuum during the dewatering cycle, when required, and for the required length of time.
- After the 300s cycle is completed, stop the filter, remove the filter cake and weigh the wet cake.
- Determine the residual moisture of the filter cake, using the SABS 924 method. This requires drying the filter cake in a vacuum oven at 105°C and 30kPa vacuum for a duration of 75 minutes.
- The final stage is to weigh the dry filter cake after it has cooled down, and store the used coal.

CHAPTER 4

RESULTS AND DISCUSSION

Throughout this project, a method of progressive planning was used. This means that the results obtained previously determined subsequent experimental work. In this chapter only the most important results, as well as the results obtain from the preparation work will be dealt with. For detailed results, the reader is referred to the CD-ROM.

4.1 Introduction

Because this was a study of a novel method of dewatering fine coal, it was difficult to devise an experimental procedure beforehand. Therefore, it was decided to use a progressive method. This means that the next type of work to be embarked upon, was determined by the results obtained in previous experiments.

The main focal point of this project, namely to show that an interruption in the applied vacuum during the dewatering cycle will give a drier final product, was constantly kept in mind.

Conclusive results were obtained. The hypothesis was proved, and a possible answer to the all-important question of why this phenomenon occurred, was found. The full results of all experiments are available on the included CD, while the averages of the values obtained are reported in Appendix A.

4.2 Preparation work

4.2.2 Particle size analysis

The particle size analyses performed, also served as a check for the validity of the splitting method. Five independent tests were done, and the results are given in Figure 4.1.

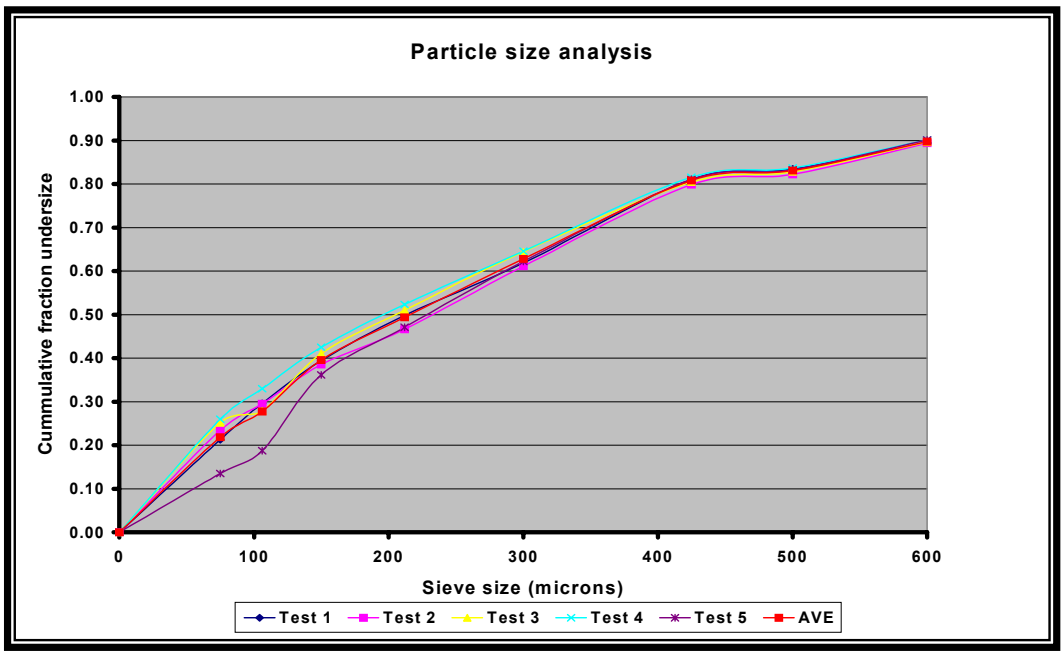

Figure 4.1: Particle size analysis.

From the graph in Figure 4.1, it is clear that the five independent tests gave substantially similar results. This also indicates that the method used to split the samples satisfied the set criteria. Another conclusion is that, on the average, the samples consisted of 27.6% -106µm particles and 49.4% -212µm particles. The importance of these fractions is stressed by the fact that the finer particles are more difficult to dewater. A detailed report of each analysis can be found in Appendix B.

4.2.2 Proximate analysis

The proximate analysis was done as described in Paragraph 3.3.3. The results of each test are given in Table 4.1.

Table 4.1: Proximate analysis results.

Test	Results
% Moisture (SABS 924)	5.13%
% Ash (ISO 1171)	46.44%
% Volatile matter (ISO 562)	17.99%
% Fixed carbon	30.44%
Calorific value	12.72 kJ/kg^{-1}

From the results of the proximate analysis, it is evident that the coal had a high ash content, which led to high final moisture levels.

4.3 Optimising results

The first group of experiments was performed mainly to prove the validity of the hypothesis. A noticeable improvement in the final moisture content of the filter cake would signal the success of the new method of dewatering fine coal. With this objective in mind, a break duration time of 30s was decided on, with three different initial break times, namely after 15s, 30s and 45s. The results are shown in Figure 4.2.

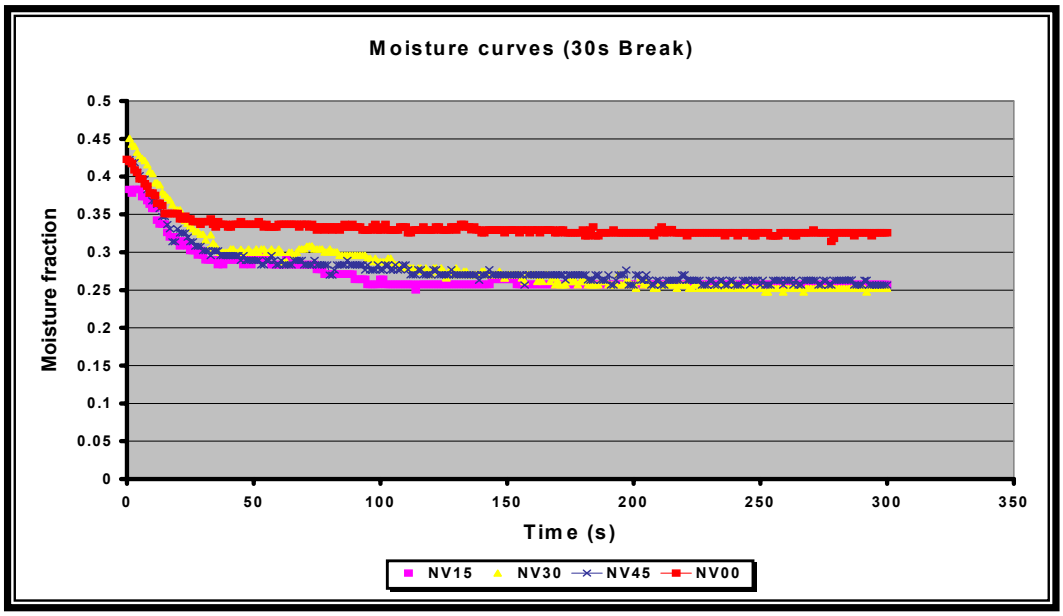

Figure 4.2: Initial results for the 30s break duration tests.

From Figure 4.2 it is clear that there was an improvement in the final moisture content of the coal filter cake. The kinetics of dewatering also improved, which results in a drier final product in a shorter time. This observation is valuable in sustaining the initial hypothesis. Note that each one of the lines in the graph represents an average value of three independent experiments.

Figure 4.2 provides two important insights. The first is that the initial slopes of the graphs are the same for all four lines. This indicates that during the funicular state the initial rate of dewatering is the same for all four cases. The second insight is that the final moisture content differed substantially for the different runs. Three of the lines indicated roughly the same final moisture content, while a much higher final moisture content was found in one run.

Considering each line in Figure 4.2 individually: The base graph (NV00) represents the dewatering at New Vaal Collieries. It is a 300s dewatering cycle with no interruptions in the applied vacuum. The final average percentage moisture determined in this test is 32.58%. The reason for the high moisture content is the high ash fraction associated with the coal. As was shown in Table 4.1, the ash content of the sample was 46.4%, as determined by the ISO 1711 method.

Consider the kinetics of the base graph in Figure 4.2: The slope in the funicular state is approximately the same as that of the other graphs. This indicates that the rate of dewatering is the same as that found in the other cases. At longer times the graph points to the pendular state, remaining almost constant from about 30s onwards, and indicating the loss of only about 1.5% moisture over the rest of the cycle.

Graph (NV15) (Figure 4.2) also shows the same slope in the funicular state. Here the applied vacuum was interrupted during the funicular state. At this point, the filter cake was dewatered to about the same moisture level as that shown by the base graph. A temporary pendular state that coincides with the one shown by the base graph, is found. As soon as vacuum is reapplied, another funicular state is created. It then moves gradually into a final pendular state and stays there for the remainder of the cycle.

The creation of the second funicular state caused additional moisture to be removed from the filter cake, leaving the filter cake with a lower final moisture content than is found without any interruptions in the applied vacuum. In this regard a final percentage moisture of 26.3% has to be compared with 32.6%.

The same kinetic trends were visible at the 30s and 45s initial break time graphs. They all had the same slope during the first funicular state, formed a temporary pendular state, and then a second funicular state in which additional water was removed. The final percentage moisture (25.23% for 30s and 27.36% for 45s) of the cakes were very similar to the one of the 15s initial break time experiments.

The final moisture contents of the three groups of tests where the vacuum application was interrupted, showed a time dependency. Keeping that in mind, an array of experiments was conducted, using different initial break times. Continuing from the previous group of tests, the initial break time was shifted with 15s intervals.

These tests showed the same tendencies as the ones discussed above. They showed the temporary pendular state and second funicular state, but all at different times in the dewatering cycle, depending on the value of the initial break time. The results of each of these tests are available on the CD-ROM. To determine whether the effect of the initial break time was time-dependent, the final percentages moisture were plotted against the initial break time. This showed the optimum point where the interruption in applied vacuum should take place. The results of these tests are shown in Figure 4.3.

From the graph in Figure 4.3, it is clear that, possibly, an optimum initial break time occurred in the vicinity of 30s. This is a definite indication that the effect of initial break time is time-dependent. What was still unknown was whether the break duration time had an influence on the optimum dewatering level.

Two reasons for the time-dependency seem plausible. The first is a structural change in the coal filter cake, and the second the possibility of water diffusion from the smaller capillaries to the larger ones, during the interruption in vacuum.

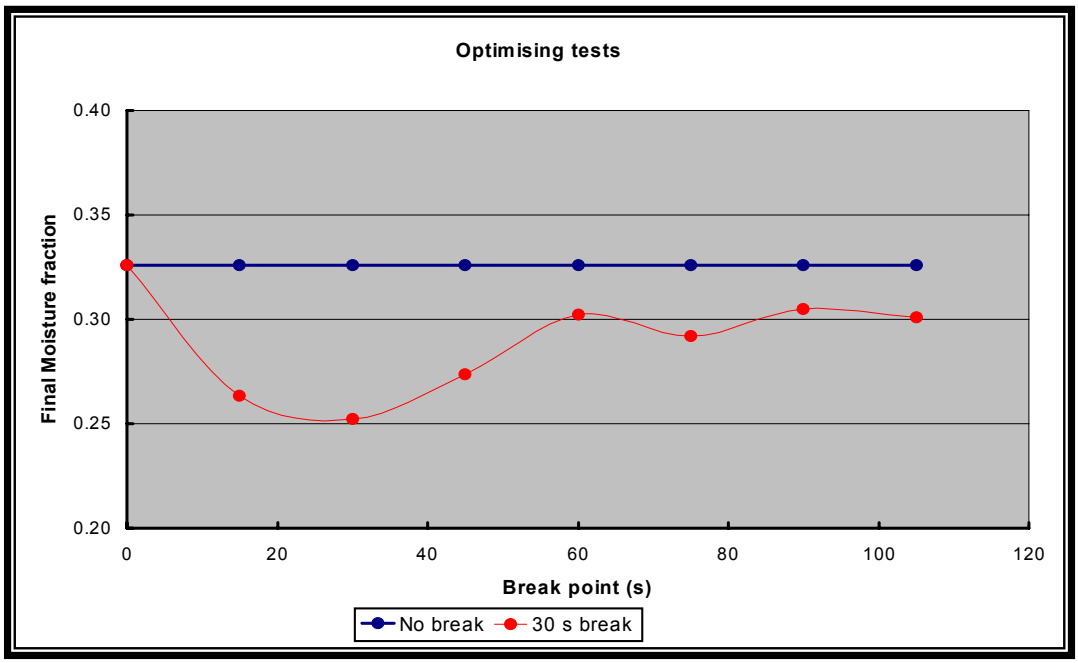

Figure 4.3: Test results for optimising the initial break time.

If a change in the structure of the filter cake occurs, this change will have to be rapid. It might be that the cake relaxes during the interruption, thus opening up some of the smaller pores and allowing water to flow to the larger capillaries. Therefore, when vacuum is reapplied the water is drawn from the larger capillaries as an additional amount of filtrate. A 15s break duration will give the same results as the 30s break duration if an actual change in the structure of the cake does indeed occur.

On the other hand, if the extra water were pulled from the cake by means of diffusion, time is of the utmost importance. Because diffusion is time dependent, the longer the time allowed for the diffusion to take place, the more water will diffuse to the larger pores, until equilibrium is reached again. A re-application of the vacuum will then draw the excess water from the filter cake. Allowing for a 60s break duration, water removal would at least be equal to that obtained with the 30s break duration tests.

4.4 Testing for water phase changes and cake structural changes

A series of tests were conducted, as for the 30s break duration tests, but using 15s and 60s break duration times instead. A graph comparing the three scenarios for a 30s initial break time is shown in Figure 4.4.

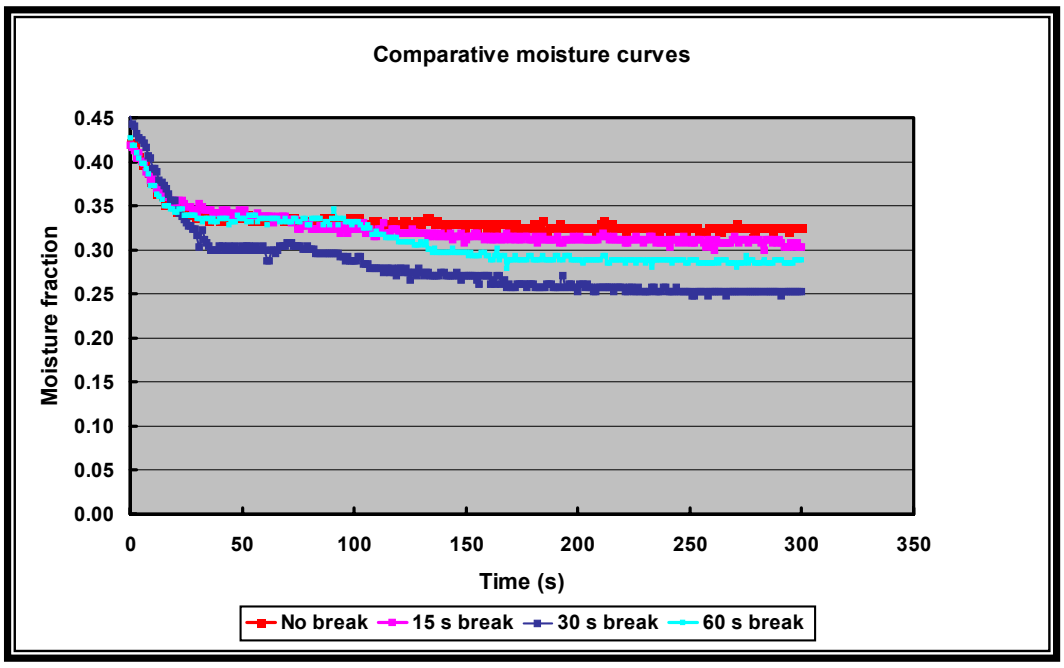

Figure 4.4: Comparative moisture curves.

From Figure 4.4 it is clear that the same tendencies were obtained as for the 30s break duration tests. Again the forming of a temporary pendular state (after the interruption of vacuum) followed by a second funicular state was present. What is interesting in this graph, is that neither the 15s break duration nor the 60s break duration tests give the same final moisture as the 30s break duration tests. This might indicate that either there is no change in the structure of the filter cake, or any diffusion of water to larger capillaries, or that the optimum break time for both these groups of tests have shifted.

In order to check for an optimum initial break time for both these methods, the final moisture content for the 15s break duration and the 60s break duration tests were plotted against initial break times, and compared to the graph in Figure 4.2. The results are displayed in Figure 4.5.

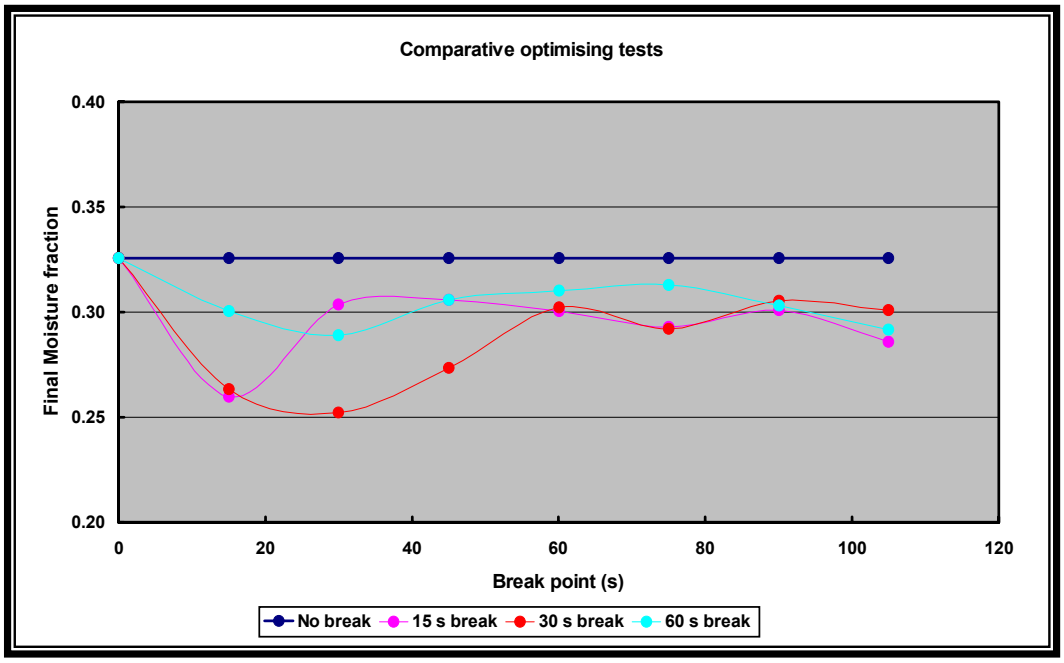

Figure 4.5: Comparative optimising tests.

Figure 4.5 shows that there is an optimum initial breaking time for both sets of experiments. The 60s break duration test's optimum breaking time is the same as the 30s break duration's, but the final moisture content differs substantially. It suggests by breaking the vacuum for too long, the moisture reaches a state of equilibrium which makes removal of the filter cake difficult. Therefore, even though it shows an optimum at 30s, the final product moisture content is much higher than expected.

4.4.1 Water phase changes

Water can undergo a phase change when the pressure exerted on it changes. In this regard, a common equation used is the Antoine equation. Before employing the Antoine equation, it is important to establish if this equation is relevant to the present investigation. It will therefore be derived from basic principles.

Refer to the PT diagram in Figure 4.6. It shows curves representing phase boundaries for a pure substance. A phase transition at constant pressure and temperature occurs whenever one of these lines is crossed, and as a result the molar or specific values of

the extensive thermodynamic properties change abruptly. Thus the molar op specific volume of a saturated liquid is very different from that for saturated vapour at the same T and P. This is true as well for internal energy, enthalpy and entropy. The exception is the molar or specific Gibbs energy which, for a pure species, does not change during a phase transition such as melting, vaporisation or sublimation.

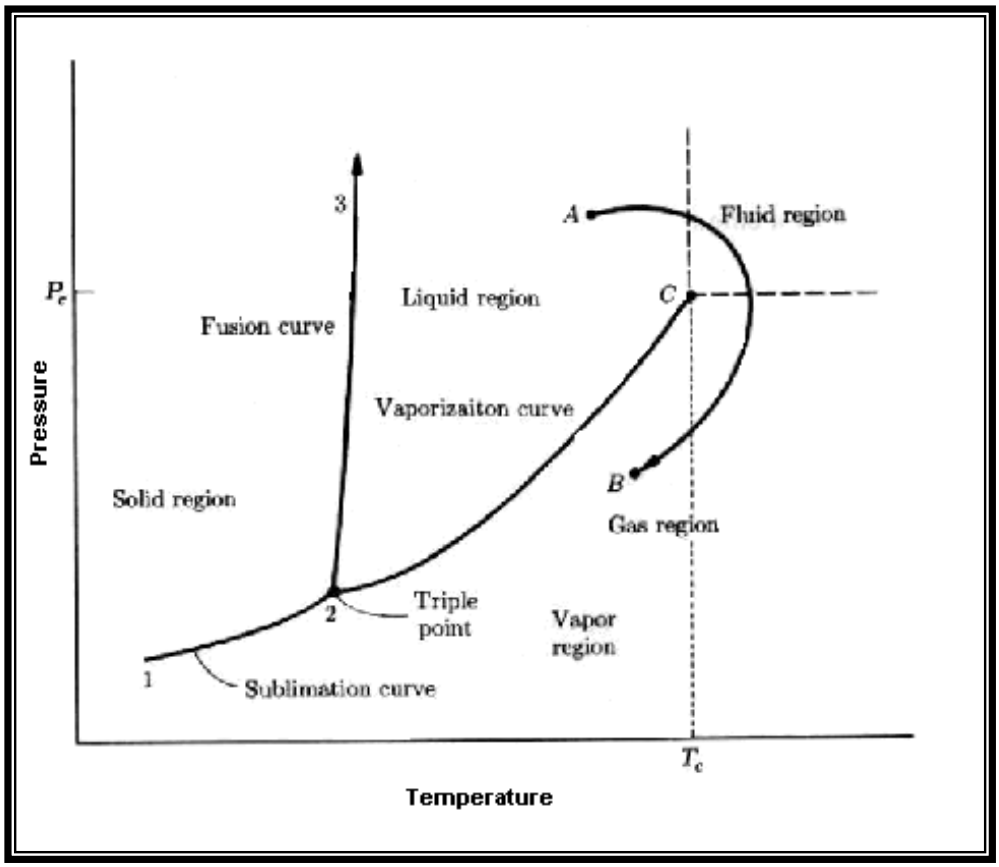

Figure 4.6: P-T diagram of water.

Consider a pure liquid in equilibrium with its vapour in a piston / capillary arrangement at temperature T and the corresponding vapour pressure P^{sat}. When a differential amount of liquid is caused to evaporate at constant temperature and pressure, Equation 4.1 applied to the process reduces to d(nG) = 0.

$$d(nG) = (nV)dP - (nS)dT \qquad (4.1)$$

Since the number of moles, n, is constant, dG = 0, and this requires the molar (or specific) Gibbs energy of the vapour to be identical with that of the liquid. More generally, for two phases α and β of a pure species coexisting at equilibrium,

$$G^{\alpha} = G^{\beta} \tag{4.2}$$

where G^{α} and G^{β} are the molar Gibbs energies of the individual phases.

The Clapeyron equation follows from this equality. If the temperature of a two-phase system is changed, then the pressure must also change in accord with the relation between vapour pressure and temperature if the two phases continue to coexist in equilibrium. Since Equation 4.2 holds throughout this change, it gives

$$dG^{\alpha} = dG^{\beta} \tag{4.3}$$

Substituting

$$dG = VdP - SdT \tag{4.4}$$

into equation 4.2 for dG^{α} and dG^{β} yields

$$V^{\alpha} dP^{sat} - S^{\alpha} dT = V^{\beta} dP^{sat} - S^{\beta} dT \tag{4.5}$$

which upon rearrangement becomes

$$\frac{dP^{sat}}{dT} = \frac{S^{\beta} - S^{\alpha}}{V^{\beta} - V^{\alpha}} = \frac{\Delta S^{\alpha\beta}}{\Delta V^{\alpha\beta}} \tag{4.6}$$

The entropy change $\Delta S^{\alpha\beta}$ and the volume change $\Delta V^{\alpha\beta}$ are the changes which occur when a unit amount of pure chemical species is transferred from phase α to phase β at the equilibrium temperature and pressure. Integration of the enthalpy equation

$$dH = Tds + VdP \tag{4.7}$$

for this change yields the latent heat of phase transition

$$\Delta H^{\alpha\beta} = T\Delta S^{\alpha\beta} \tag{4.8}$$

Thus $\Delta S^{\alpha\beta} = \Delta H^{\alpha\beta} / T$, and substitution in Equation 4.6 gives

$$\frac{dP^{sat}}{dT} = \frac{\Delta H^{\alpha\beta}}{T\Delta V^{\alpha\beta}} \tag{4.9}$$

which is the Clapeyron equation. For the particularly important case of phase transition from liquid *l* to vapour *v*, it is written as

$$\frac{dP^{sat}}{dT} = \frac{\Delta H^{lv}}{T\Delta V^{lv}} \tag{4.10}$$

Assuming that

$$\Delta V^{lv} = V^{v} = \frac{RT}{P^{sat}} \tag{4.11}$$

Equation 4.10 becomes

$$\frac{dP^{sat}}{dT} = \frac{\Delta H^{lv}}{RT^2 / P^{sat}} \tag{4.12}$$

Rearrangement of Equation 4.12 yields the equation known as the Clausius/Clapeyron Equation (4.13).

$$\Delta H^{lv} = -R \frac{d \ln P^{sat}}{d(1/T)} \tag{4.13}$$

Equation 4.13 shows that ΔH^{lv} is proportional to the slope of a plot of ln P^{sat} vs. 1/T. Experimental data for many substances show that such plots produce lines that are nearly straight. This then implies that ΔH^{lv} is almost constant and independent of T. This, however, is not true. The assumption on which the Clausius/Clapeyron equation is based has approximate validity only at low pressures.

Since a plot of ln P^{sat} vs. 1/T generally yields a line that is nearly straight, i.e.,

$$\ln P^{sat} = A - \frac{B}{T} \tag{4.14}$$

where A and B are constants for a given species. This equation gives a rough approximation of the vapour-pressure relation for the entire temperature range from the triple point to the critical point. Moreover, it provides an excellent basis for interpolation between values that are reasonably spaced.

The Antoine equation, which is more satisfactory for general use, has the form (Smith, Van Ness & Abbott, 1996: 31-34)

$$\ln P^{sat} = A - \frac{B}{T + C} \tag{4.15}$$

A principal advantage of this equation is that values of the constants A, B and C are readily available for a large number of species, including water. Each set of constants is valid for a specified range, and should not be used outside of that range.

Using the values for A = 18.3036, B = 3816.44 and C = -46.13 (Himmelblau, 1996), it was determined that for a sudden increase in pressure of 45 kPa, the temperature will increase by 78.73°C. If one assumes that the room temperature is about 22°C (most work was done in the winter and in the shade) it is easy to see that if there is a sudden release of vacuum back to atmospheric level, the temperature will increase to about 100°C. This could indicate that an amount of water evaporates when the vacuum is released. This vapour could then diffuse from the smaller capillaries to the larger capillaries, condensing in the larger capillaries. When the vacuum is reapplied, the water is drawn from the larger pores to result in a drier cake.

This was easy to test experimentally. If one introduces more than one interruption to the applied vacuum during a dewatering cycle, the end result must be better than for a single interruption in vacuum. It must be kept in mind, though, that there is a time delay for the system to again reach 45 kPa. This must be brought into the equation. The results of these experiments are shown in Figure 4.7.

The first thing to note is that the final moisture content of the tests were all much higher than in previous cases. Although it was better than for the base graph (indicated in red) it was not as good as for the tests with a single interruption in vacuum.

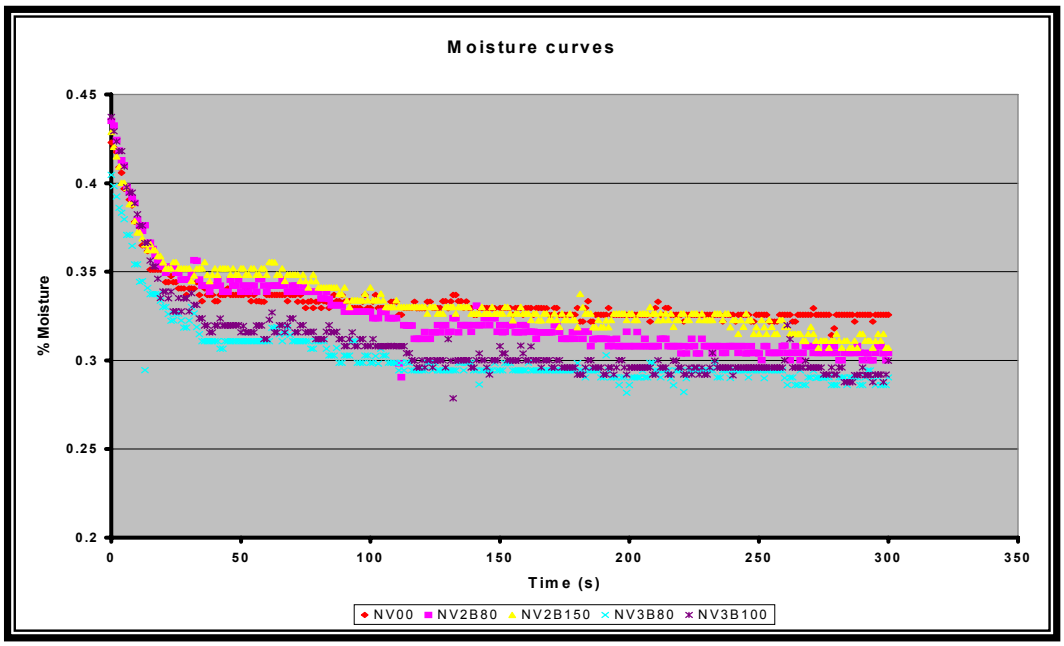

Figure 4.7: Repeated breaks in vacuum.

All the similarities of the previous tests were again observed, namely an initial funicular state, having a similar rate of dewatering, and the forming of a temporary pendular state, followed by another funicular state and, finally, a pendular state. What is notable, is the absence of more temporary pendular states, when the vacuum was interrupted more than once.

From the information in Figure 4.7, it was safe to rule out evaporation followed by diffusion as a cause for a drier final filter cake.

4.4.2 Structural changes

In Figure 4.5, the 15s break duration tests showed an optimum much earlier than the other two sets of experiments. What is also important to notice, is that the final moisture content is in the vicinity of that of the 30s break duration tests. This might be an indication that there is a possible structural change in the form of cake compressibility and/or area changes.

4.4.2.1 Compressibility

The compressibility of coal filter cakes was tested, and although the validity of the results is unknown, the results could be interpreted to be in agreement with theory. Figure 4.8 shows these results.

Figure 4.8 is a graph of the specific cake resistance (α) vs. the log of the applied vacuum (ΔP). For incompressible filter cakes, these graphs are supposed to show horizontal lines. It is clear that the expected results were not obtained.

Considering the model of pressure drop in a filter cake, the following relationship can be derived:

Flow of filtrate through a filter cake can be treated as flow through a packed bed. Equation 4.16 describes these flow conditions.

$$f_b = \frac{150(1-\varepsilon)}{Re_p} + 1.75 \qquad (4.16)$$

In most practical cases, the flow is laminar and consequently the Carman-Kozeny equation (4.17) can be adapted (4.18).

$$f_b = \frac{150(1-\varepsilon)}{Re_p} \qquad (4.17)$$

$$\frac{\Delta P}{L} = \frac{150(1-\varepsilon)^2 \mu v_s}{\varepsilon^3 d_{vs}^2} \qquad (4.18)$$

This equation relates the drop in pressure to the porosity and thickness of the cake, and to the particle diameter. However, to allow for more measurable filtration parameters, the equation has to be modified. Firstly the particle size is expressed in terms of the specific surface area, given by

$$d_{vs} = \frac{6}{S_p / V_p} = \frac{6}{S_0} \qquad (4.19)$$

Provisionally, the cake thickness L can be expressed in terms of the mass of cake M_c,

$$M_c = \rho_s (1-\varepsilon) A_c L \qquad (4.20)$$

Combining Equations 4.18 – 4.20:

$$\begin{aligned}\Delta P &= \frac{4.17\mu v_s M_c S_0^2 (1-\varepsilon)}{A_c \rho_s \varepsilon^3} \\ &= \mu v_s \cdot \frac{\alpha M_c}{A_c}\end{aligned} \tag{4.21}$$

where α is the specific cake resistance, defined as

$$\alpha = \frac{4.17(1-\varepsilon)S_0^2}{\rho_s \varepsilon^3} \tag{4.22}$$

The grouping of terms describing the filter cake properties into specific cake resistance does not imply that α will be constant for any given slurry. When α is insensitive to ΔP, the filter cake is described as incompressible, although probably no cake is actually this ideal. Even for a constant pressure drop ΔP, α may change because of variations in the void fraction ε and the specific surface S_0 (Kelly & Spottiswood, 1997: 343-366).

The filtration pressure drop ΔP_f also must overcome the resistance of the filter medium, which is in series with the cake resistance. Since Equation 4.21 is in the familiar form of a driving force proportional to a resistance times a rate, the medium resistance Ω_m can be included in the equation to give

$$\Delta P_f = \Delta P_c + \Delta P_m = \mu v_s \left(\frac{\alpha M_c}{A_c} + \Omega_m \right) \tag{4.23}$$

In filtration it is generally more convenient to have the superficial velocity v_s and the total mass of cake M_c expressed in term of V_f, the total volume of filtrate collected. Thus,

$$v_s = \frac{dV_f}{dt}\frac{1}{A_c} \tag{4.24}$$

A mass balance may be used to relate M_c and V_f. If the feed slurry is dilute

$$M_c = V_f C_c \tag{4.25}$$

(C_c = the mass of solids deposited as cake per unit volume of filtrate collected). In reality some of the filtrate stays behind in the pores of the cake so that the filtrate

collected is less than the water in the feed slurry. This results in C_c being greater than the concentration of solids per unit volume in the feed slurry C_I. A rigorous mass balance therefore results in the correction

$$C_c = \frac{C_I}{1 - (M_{we} / M_c - 1)(C_I / \rho_l)} \tag{4.26}$$

(M_{we} = the mass of the wet cake, including pore liquid; ρ_l = density of the filtrate). Combining equations 4.23 – 4.25 gives:

$$\Delta P_f = \frac{dV_f}{dt}\frac{\mu}{A_c}\left(\frac{\alpha C_c V_f}{A_c} + \Omega_m\right) \tag{4.27}$$

or

$$\Delta P_f = \frac{dV_f}{dt}\frac{\alpha C_c \mu}{A_c^2}(V_f + V_e) \tag{4.28}$$

(V_e = volume of filtrate necessary to build up a fictitious amount of filter cake, the resistance of which is equal to the filter medium and the piping between the pressure tapping points).

Most filter cakes are, to some extent, compressible. By conducting constant pressure experiments at various pressure drops, the variation of α with ΔP_f may be found. A number of empirical equations have been presented, but the most widely used is

$$\alpha = \alpha_0 (\Delta P_f)^n \tag{4.29}$$

where α_0 and n are empirical constants: the latter being called the compressibility coefficient. For incompressible filter cakes the value of the compressibility constant is zero, but is usually between 0.2 and 0.8 (Kelly & Spottiswood, 1997: 343-366).

Experimentally, a plot of $\ln(\alpha)$ vs $\ln(\Delta P_f)$ should yield a horizontal line for incompressible filter cakes. This was done, and the results are shown in Figure 4.8 for two different cake thicknesses (Kukard, 2001).

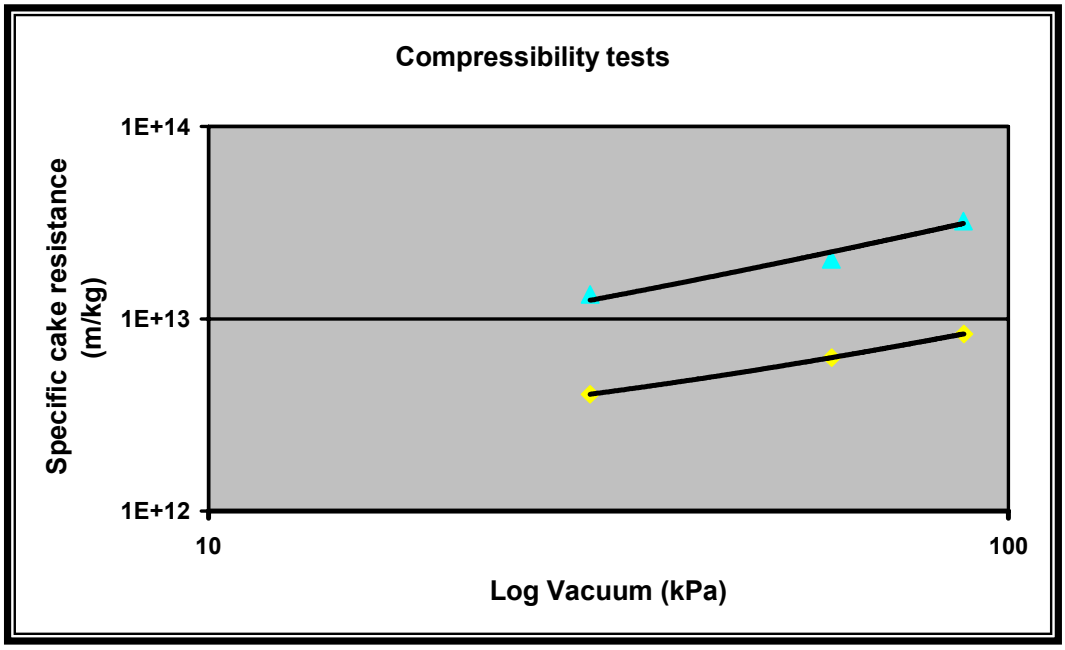

Figure 4.8: Compressibility tests.

Form the graph in Figure 4.8 it can be seen that the lines are not entirely horizontal. This means that the filter cakes show some compressibility, which might be because of the void fractions and specific surfaces as discussed above. It must be kept in mind that the y-axis is zoomed in. If one utilises the whole array of values, the lines will be more horizontal. Therefore, it is safe to rule out the possibility of compressibility and relaxation of the filter cake. This is in agreement with the literature found on this subject (Gala, Kakwani, Chiang, Tierney & Klinzing, 1981: 1611-1632).

4.4.2.2 Area changes

The structural changes that may be expected might be in the form of cracks at the bottom of the filter cake. This might explain why the moisture level is so high in the 60s break duration experiments. It could be that the cracks open up to such an extent that there is a loss in vacuum over the filter cake. Such behaviour, though, was not observed and it was expected that the amount of cracking was not the same during the 60s break duration experiments.

This theory was easy to explain. Cracking of the filter cake took place after the vacuum was reapplied. In the case of the 15s and 30s break duration experiments the vacuum was reapplied at a stage where the filter cake did not get much time to dry in the air. There was an optimum amount of air-drying that had to take place, and that was between 15s and 30s. After 30s of air-drying, the filter cake got too dry, causing a decreasing surface tension. After reapplying the vacuum, the cake was much more prone to cracking, and thus ended up with a surface that cracked more and formed more fine particles. These particles then settled down between the coarser particles, blocking the opened pores and in effect decreasing the newly formed pore sizes. This then led to greater capillary pressures and thus decreasing the chance of dewatering the coal filter cake.

The question that remained was if this assumption could be verified and explained, both mathematically and experimentally. It was found to be possible.

Consider the matter from a mathematical point of view. Although filtration is only one-phase flow, in comparison with two-phase flow during dewatering, it was felt that, since dewatering models are very difficult to solve (see Section 4.4.2.3), a simple filtration model might be used to explain the occurrences. The model that was decided upon, was Darcy's model for filtration (4.30). It describes the flow of a wetting fluid through a bed during cake formation, and is written as follows:

$$\frac{dv}{dt} = \frac{KA\Delta P}{\eta L} \qquad (4.30)$$

where dv/dt is the rate of filtrate flow and ΔP is the pressure difference across the cake.

Integrating equation 4.30 and rearranging, yields Equation 4.31:

$$\frac{t}{v} = \frac{\eta C_c}{2A^2 \Delta P K \rho_s (1-\varepsilon)} v + \frac{R_m \eta}{A \Delta P} \qquad (4.31)$$

where C_c is the ratio of mass of solid to volume of filtrate produced during cake formation, ρ_s is the density of the solids, ε is the cake porosity and R_m is the resistance of the filter medium (Condie & Veal, 1998: 1-34).

Rearranging Equation 4.31 and writing it in terms of the amount of filtrate that flows through the cake, Equation 4.32 was obtained. From this equation the assumption of increasing area could be proven.

$$v = \frac{2tA^2\Delta PK\rho_s(1-\varepsilon)}{\eta C_c v + 2R_m\eta AK\rho_s(1-\varepsilon)} \quad (4.32)$$

Giving all the variables that remained constant throughout all the experiments a value of 1, Equation 4.32 was reduced to yield only the variables that had an influence on each of the individual experiments. The constant variables were defined as follows:

- $t = 1$: The time duration for all the experiments was the same.
- $\Delta P = 1$: The experiments were conducted at constant pressure of 45kPa.
- $C = 0$: The cake was formed under hindered settling, and therefore no filtrate was produced during cake formation. The first term in the denominator thus reduces to zero.
- $R_m = 1$: The same filter medium was used in every experiment.
- $\eta = 1$: The viscosity of the fluid was the same, as the same tap water was used in all experiments.
- $K = 1$, $\rho_s = 1$: The same coal sample was used in all experiments, which means that if the sampling method was correct, the permeability and density of the solids were the same in all experiments. This was the case, as shown in Section 4.1.

Equation 4.32 therefore reduced to the following:

$$v = \frac{A^2(1-\varepsilon)}{A(1-\varepsilon)} \quad (4.33)$$

Equation 4.33 could be reduced further to

$$v \propto A \quad (4.34)$$

This means that the amount of filtrate gathered during filtration, and in this case dewatering, was proportional to the area of the filter cake in contact with the vacuum. It also shows that the rate of airflow through the cake has a major influence on the dewatering of the cake. Therefore, increasing the area by means of cracking the filter cake would increase the airflow through the cake and would consequently produce a drier final product.

Figure 4.9: The broken filter cake.

In order to obtain empirical verification, an experiment was conducted in which there were no adjustments of the vacuum (neither step changes, nor interruptions). After 30s of desaturation, the filter cake was broken using a spatula, causing two parallel, artificially created "cracks", as shown in Figure 4.9.

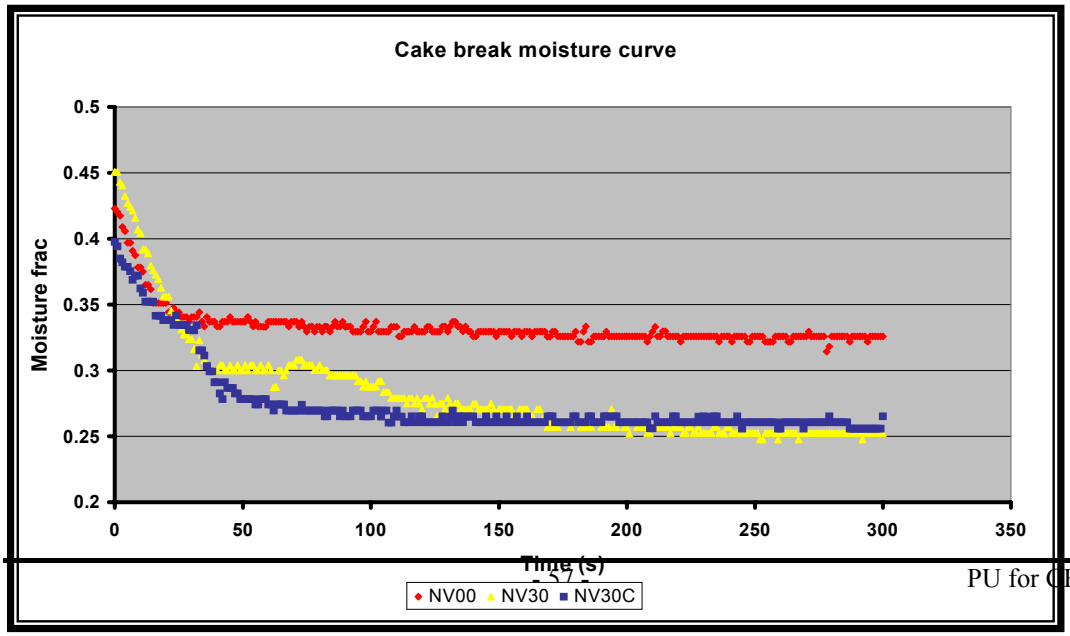

Figure 4.10: Cake break experiment.

The result of these experiments is shown in Figure 4.10. It shows a graph that compares very favourably with the results of the 30s break experiments. In the figure, the base test is indicated by the red line, the experiment where the cake was broken by the blue, and the experiment for a 30s initial vacuum break- and break duration time by the yellow. All three these experiments showed a similar funicular state. The difference is apparent in the forming of the pendular state.

The base graph shows a pendular state, which remains until the end of the tests, as was expected. The 30s break graph displays the temporary pendular state, followed by the second funicular and pendular states. The graph for the experiment where the cake was broken, initially indicated a pendular state, very similar to the base graph, just before the cake was punctured. A return to the funicular state is then shown, with a much steeper slope. This means that the rate of dewatering of the cake is much higher than for the other cases. It is evident that a final pendular state is reached much quicker than in any of the other tests.

It means that a punctured filter cake would firstly give a drier final product, and secondly, would dry out at a rate that is much greater than by any of the other methods. The question of the airflow rate could not be negated at this stage, as it did have an influence on the kinetics of the dewatering.

Another aspect that was kept in mind, was the reduction of the vacuum. Whenever a filter cake cracked, whether induced or by accident, the applied vacuum decreased accordingly. This implied that there must have been an optimum amount of cracking, before the applied vacuum became insufficiently low. A reduction of about 35% in the applied vacuum, however, did not exert a negative influence on the dewatering rate.

4.4.2.3 Difficulties using Wakeman's model

In Section 2.4 it was suggested to use Wakeman's model as the backbone for this project. Studying this model showed that it was to difficult to solve, making it virtually impossible to apply to this work.

Solving Wakeman's model involves the simultaneous solution of four partial differential equations (Appendix D), a technique far too complicated for the purpose of this project. In fact, the technique in solving Wakeman's model is so complicated that, to date, only two papers were found that indicated how this model was solved (Wakeman, 1978:655-669 and Condie & Veal, 1998: 1-34). In both cases, no solution methodology was given. Both papers only printed the results and graphical findings.

For these reasons it was decided to compare the theory developed in the laboratory to a much simpler model. Darcy's law was the obvious choice because of its simplicity to use, and its accuracy in describing filtration systems.

4.5 Ultra fine tests

By sieving the control sample to -212μm, tests were conducted using only ultra fine coal. Unfortunately the aperture of the filter cloth was too coarse, allowing about 70% of the ultra fine coal to pass through the cloth. This led to a filter cake about 3mm thick, which was insufficient for proper tests. To be able to test ultra fines, a membrane must be used as filter medium.

CHAPTER 5

CONCLUSIONS AND RECOMMENDATIONS

In this chapter, conclusions drawn from the experimental results will be presented, together with a short assessment of the validity of every conclusion. Finally some relevant recommendations will be made to further develop this project and to get the best results achievable.

5.1 Conclusions

- The first conclusion to be drawn from this work is that the hypothesis made at the outset was correct. This means that there is a definite improvement in the final moisture of a fine coal filter cake if an interruption in the applied vacuum is introduced during a dewatering cycle. It does not necessarily mean that the improvement is due to the interruption in the vacuum, but it is a result of several occurrences when the interruption is introduced.

- The vacuum interruption is time-dependent. This is a twofold dependency which means that it is dependent on both the time in the cycle that the interruption occurs, as well as the length of the break time. Further studies of the time dependency showed an optimum initial break time at 30s into the dewatering cycle. This optimum occurred for both instances where the applied vacuum was interrupted for the duration of 30s and 60s. For a break duration of 15s, the optimum was shown to be at the 15s initial break time.

  Since the time-dependency has two aspects, the break duration time should be taken into account as well. This implies that the point where the initial break time, and the break duration time show the lowest final moisture percentage, defines the optimum time combination. This point was established for an initial break time of about 29s and a break duration time of 30s.

- When a system is placed under 45 kPa of vacuum, it decreases the effective boiling temperature of water by 78°C. In short this means that the water in the system, and in this case the filter cake, will evaporate. In a filter cake, this water vapour can diffuse from smaller capillaries to larger capillaries. When the vacuum is broken, the effective temperature of the system drops back to room temperature, and the water vapour will then condense in the larger capillaries. A reapplication of the vacuum can ultimately withdraw an extra amount of water.

  A mathematical basis for the above observations was sought by using the Antoine equation for phase changes. The Antoine equation is, however, not suitable for vacuum systems, and consequently a method of interpolation was used to evaluate the new effective temperature values.

  The test for this type of occurrence also showed negative results. It might be due to the fact that the filter cake has a pressure gradient across it, which means that not all the water in the cake will evaporate, if any at all. To test the possibility of removal of water using diffusion, the whole filter cake should be subjected to the same level of vacuum.

  It is thus safe to rule out this explanation as to why a drier filter cake is obtained by breaking the vacuum during a dewatering cycle.

- A better explanation is based on structural changes in the filter cake during the vacuum break. Using Darcy's law for one phase flow, it was shown that the amount of filtrate gathered is proportional to the area of the filter cake subjected to the vacuum, as well as the airflow through the cake. Although working with two phase flow systems, the assumption was made that the area subjected to the vacuum will play almost the same role as for one phase flow. Therefore, if the area of the filter cake can be increased in the vertical direction, better dewatering will be possible.

  Since dewatering is a two-phase flow system, the influence of airflow through the cake cannot be ignored. Looking at it logically, it is easy to reason that if the

cake area increases too much in a vertical direction, the loss of vacuum will be too large to compensate for an increase in the area of the filter cake. Consequently the amount by which the area of a filter cake is increased, is dependent on the amount of vacuum loss.

Experimentally it was shown that an increase in area of 1260mm^2, from 3525.65mm^2 to 4785.65mm^2, decreases the percentage moisture of the final product by approximately 7%. Conversely: a 35% increase in the area of the cake will result in a 7% decrease of the final moisture percentage. The exact relation between these two parameters is not known yet, as Darcy's law only applies to one-phase flow systems.

- Regarding structural changes - it was confirmed that a fine coal filter cake can be treated as an incompressible cake. Initially it was thought that there might be a small degree of compressibility in fine coal filter cakes. Experimental results confirmed this initial believe.

  Comparing these results with those found in the literature, it was discovered that the discrepancy in the results was due to void fractions and specific surfaces.

- Kinetics plays a key role during the improved method of dewatering. This is indicated by the fact that there is a great improvement in the rate at which the dewatering in a coal filter cake takes place. Another indication is that the new method of breaking the vacuum or, even better, the filter cake, yields better results when done in the funicular state of the dewatering process.

- When testing for the influence of ultra fine coal, a membrane and not a filter cloth should be used as filter medium.

5.2 Recommendations

- More tests should be conducted in order to find a time dependency for the breaking of the filer cake. This entails establishing if there is a specific time in the dewatering cycle at which the filter cake should be broken.

- Testing for porosity influence, using a Mercury Porosimeter, should be done on laboratory scale. These tests will have to coincide with the testing of the influence of increased airflow through the cake.

- Before trying to upgrade a final product to industry standards, more laboratory scale testing should be completed to study the relationship between increased surface area and loss of vacuum. Together with the attempt to solve Wakeman's model for two-phase flow, a model should be developed to incorporate the newly-increased surface.

- After the laboratory scale testing is complete, a small pilot plant construction is recommended as the next step in upgrading to industrial scale. This pilot scale test should concentrate on only a limited number of changes to be made to the standard vacuum belt filter and should produce results whereby only one aspect is taken to industry.

- The aspect of diffusion of water and vacuum subjected dewatering will have to receive attention. This might hold the key to all the answers for better dewatering.

- Industry application is of the utmost importance. After satisfactory results have been achieved, a device should be designed and put into place in the industry. At this stage it is proposed to design a device that has a single axis, running across the width of the filter. A number of circular blades will be fitted to the axis which run on the belt, cutting the filter cake and thus increasing the airflow and the area of the cake.

- A final proposal is to compare the results of vacuum filtration with those that include pressure filtration and centrifugation.

REFERENCES

ANON. 1986. Three new approaches to the problem of dewatering fine coal. Coal Age, **52-54**, **Jan**.

BALUAIS, G., DODDS, J.A. & TONDEUR, T. 1985. A model for the desaturation of porous media as applied to filter cakes. International Chemical Engineering, **25(3):436-446, Jul**.

BARTON, W.A. & LYNCH, L.J. 1994. Coal inherent moisture – its definition and measurement. 6th Australian Coal Science conference, Newcastle : AMF. **65-72, Oct.**

BAYLES, G.A., KLINZING, G.E. & CHIANG, S. 1989. Fractal mathematics applied to flow in porous systems. Part. Part. Syst. Charact. 6. **JKMRC : Queensland University. 168-175**.

BROWNELL, L.E. & KATZ, D.L. 1947. Flow of fluids through porous media – Single homogeneous fluids. Chemical Engineering Process, **43(10):537-548, Oct.**

BOURGEOIS, F.S., & BARTON, W.A. 1997. Advances in the fundamentals of fine coal filtration. Coal Preparation **(19):9-31**.

BOURGEOIS, F.S. & LYMAN, G.J. 1997. Morphological analysis and modelling of fine coal filter cake microstructure. Chemical Engineering Science **52(7):1151-1162**.

BUCKLEY, A.N. & NICOL, S.K. 1995. Surface related moisture retention characteristics of coal. 2nd ed. Australia : CSIRO. **1-12, May**.

CARLETON, A.J. & MACKAY, D.J. 1988. Assessment of models for predicting the dewatering of filter cakes by gas blowing. Filtration and Separation, **187-191, May/Jun**.

CHENG, Y.S., FANG, S.R., TIERNEY, J.W. & CHIANG, S.H. 1988. Application of enhanced vacuum filtration to dewatering of fine coal refuse. Separation Science Technology, **23(12&13):2113-2130**.

CHI, S., KLINZING, G.E. & CHANG, S. 1985. Effect of entrapped air bubbles on fine coal dewatering via filtration. Powder Technology, **45:25-34**.

CONDIE, D.J. & VEAL, C.J. 1997. Modelling the vacuum filtration of fine coal: Part 2. Filtration and Separation, **Nov:957-963**.

CONDIE, D. & VEAL, C., 1998. Improved fine coal dewatering via modelling of cake desaturation. Australia : CSIRO. **Apr:1-34**.

CONDIE, D.J., HINKEL, M. & VEAL, C.J. 1996. Modelling the vacuum filtration of fine coal. Filtration and Separation, **Oct:825-834**.

DULIEN, F.A.L. & MEHTA, P.N. 1971/72. Particle size and pore (void) size distribution determination by photomicrographic methods. Powder Technology, **(5):179-193**.

FRANZIDIS, J.P. 1991. Developments in fine coal benefication in South Africa. Coal Preparation, **(11):103-114**.

GALA, H.B., KAKWANI, R., CHIANG, S.H., TIERNEY, J.W. & KLINZING, G.E. 1981. Filtration and dewatering of fine coal. Separation Science Technology, **16(10):1611-1632**.

HALVORSEN, W.J. Advantages and disadvantages of dewatering fine coal. Industrial practice of fine coal processing. **239-241**.

HIMMELBLAU, D.M. 1996. Basic principles in chemical engineering. 6th ed. London. Prentice Hall. **Steam Tables.**

HORSFALL, D. W. ed. 1980. Coal preparation for plant operators. Cape Town : The South African Coal Processing Society. **306-340**.

JOHNSTON, P.R. 1998. Revisiting the most probable pore-size distribution in filter media: The gamma distribution. Filtration and Separation, **Apr:287-292**.

KAKWANI, R.M., CHIANG, S.H. & KLINZING, G.E. 1984. Effect of filter cake structure on dewatering of fine coal. Minerals and Metallurgical Processing, **Aug:113-117**.

KAKWANI, R.M., GALA, H.B., CHIANG, S.H., KLINZING, G.E. & TIERNEY, J.W. 1985. Dewatering of fine coal – Micrographic analysis of filter cake structure. Power Technology, **(41):239-250**.

KELLY, E.G. & SPOTTISWOOD, D.J. 1997. Introduction to mineral processing. 1st ed. Adelaide : Australian Minerals Foundation. **343-366**.

KUKARD, R. 2001. 'n Studie oor die saampersbaarheid van fyn steenkool-filterkoeke. Vierdejaar Skripsie, Skool vir Chemiese- en Mineraalingenieurswese. Potchefstroom : PU vir CHO.

LE ROUX, M. 2000. Die bepaling van poriegrootte-distribusie-index van fyn steenkool. Vierdejaar Skripsie, Skool vir Chemiese- en Mineraalingenieurswese. Potchefstroom : PU vir CHO.

LOCKHART, N.C. & KERN, R. 1996. Research and development needs in filtration and dewatering. Drying Technology, **14(6):1241-1264**.

MISHRA, S.K. Principles of dewatering. Industrial practice of fine coal processing, **213-221**.

PALICA, M. 1994. Mechanical dewatering of the flotation concentrate of coking coal. Chemical Engineering and Processing, **33:141-149**.

RONG, R.X. 1993. Literature review on fine coal and tailings dewatering. Advances in coal preparation technology, **(2) Project P239A**. Brisbane. Australia : JKMRC, University of Queensland. **Nov. 120p**.

RONG, R.X. & HITCHINS, J. 1993. Fine coal and tailings dewatering – Practice and performance. Advances in coal preparation technology, **(3) Project P239A**. Brisbane. Australia : JKMRC, University of Queensland. **Nov. 102p**.

RONG, R.X. & HITCHINS, J. 1994. Preliminary study of correlations between fine coal characteristics and properties and their dewatering behaviour. Brisbane. Australia: JKMRC, University of Queensland, **Nov 293-309**.

RUI, Z. 1997. Measuring the structure of fine coal filter cakes using image analysis. Ph. D. dissertation. Brisbane. Australia : JKMRC, University of Queensland. **Mar**.

RUTH, B.F. 1933. Studies in Filtration III. Derivation of general filtration equations, IV Nature of fluid flow through filter septa and its importance in the filtration equation. Ind Eng Chem., **(27):708 and 806.**

RUSHTON, A. & ARAB, M.A.A. 1989. Internal pressure variations during the filtration and dewatering of thick cakes. Filtration and Separation, **May/Jun:181-186**.

SHENG-MING, C., KLINZING, G.E., & CHANG, S. 1985. Effect of entrapped air bubbles on fine coal dewatering via filtration. Powder Technology, **(45)25-34**.

SMITH, J.M., VAN NESS, H.C. & ABBOTT, M.M. 1996. Introduction to chemical engineering thermodynamics. 5th ed. New York : McGraw-Hill. **346p**.

SNYMAN, C.P. Red. 1996. Geologie vir Suid-Afrika. Pretoria : Dept. Geologie, University of Pretoria. **608p**.

SUNG, D & PAREKH, B.K. 1996. Statistical evaluation of hyperbaric filtration for fine coal dewatering. Korean Journal of Chemical Engineering, **13(3):304-309**.

SUNG, D.J., GROPPO, J.G. & PAREKH, B.K. 1994. Cake uniformity in pressure filtration of coal slurry. Filtration and Separation, **Dec:819-824**.

TAO, D., GROPPO, J.G. & PAREKH, B.K. 2000. Enhanced ultrafine coal dewatering using flocculation filtration processes. Minerals Engineering, **13(2)163-171**.

VENKATADRI, R., CHIANG, H.S., KLINZING, G.E. & TIERNEY, J.W. 1994. A fundamental study of filtration and dewatering of fine coal. Coal preparation, **(1)71-92**.

VAN DER WALT, P.J. 1984. Coal washing in South Africa. Johannesburg : University of the Witwatersrand.

WAKEMAN, R.J. & TARLETON, E.S. 1991. Solid/liquid separation equipment simulation & design – an expert systems approach. Filtration and Separation, **Jul/Aug:268-274**.

WAKEMAN, R.J. s.a. Dewatering of filter cakes: Vacuum and pressure dewatering. Devon. U.K. : University of Exeter. **420p**.

WAKEMAN, R.J. s.a. Filtration theory: Formation and structure of compressible filter cakes. Devon. U.K. : University of Exeter. **364p**.

WAKEMAN, R.J. 1975. Filtration post-treatment processes. Chemical Engineering Monographs. ed. Churchill, S.W. Amsterdam : Elsevier Scientific Publishing Company. **75p**.

WAKEMAN, R.J. 1976. Vacuum dewatering and residual saturation of incompressible filter cakes. International Journal of Mineral Processing, **3:193-206**.

WAKEMAN, R.J. 1977. Cake dewatering. Solid/liquid Separation, **Ed. L. Svarovsky, 2nd ed:297-306**. London : Butterworths.

WAKEMAN, R.J. 1978. The performance of filtration post-treatment processes, 1. The prediction and calculation of cake dewatering characteristics. Filtration and Separation, **Nov/Dec:655-669**.

WAKEMAN, R.J. 1979. Low-pressure dewatering kinetics of incompressible filter cakes, I. Variable total pressure loss or low-capacity systems. International Journal of Mineral Processing, **5:379-393**.

WAKEMAN, R.J. 1979. Low-pressure dewatering kinetics of incompressible filter cakes, II. Constant total pressure loss or high capacity systems. International Journal of Mineral Processing, **5:395-405**.

WAKEMAN, R.J. 1982. An improved analysis for the forced gas deliquoring of filter cakes and porous media. Journal of Separation process technology, **3(1):32-38**.

WAKEMAN, R.J. 1984. Residual saturation and dewatering of fine coals and filter cakes. Powder Technology, **(40):53-63**.

WALKER, A.J. & SVAROVSKY, L. 1994. Development of a computer model for predicting the filtration characteristics of a suspension. Filtration and Separation, **Jan/Feb:57-65.**

WOOLLACOTT, L.C. & ERIC, R.H. 1994. Mineral and metal extraction: an overview. 1st ed. Johannesburg : SAIMM. **364p**.

EXPERIMENTAL SCHEDULE

APPENDIX A

A.1 General

A sample was gathered upstream from the flocculant addition point at New Vaal Collieries. This sample was then taken to Potchefstroom University. Here the sample was first conditioned, then split into the relevant groups after which a particle size analysis was done on the coal. The final stage of pre-testing was to do a proximate analysis on the coal sample.

A.2 15s break duration experiments

Table A.1 is an indication of the schedule for the 15s break duration experiments.

Table A.1: 15s break duration experimental schedule.

Test No.	Break time	Break duration	Test No.	Break time	Break duration
NV00E1	0s	-	NV60E1	60s	15s
NV00E2	0s	-	NV60E2	60s	15s
NV00E3	0s	-	NV60E3	60s	15s
NV15E1	15s	15s	NV75E1	75s	15s
NV15E2	15s	15s	NV75E2	75s	15s
NV15E3	15s	15s	NV75E3	75s	15s
NV30E1	30s	15s	NV90E1	90s	15s
NV30E2	30s	15s	NV90E2	90s	15s
NV30E3	30s	15s	NV90E3	90s	15s
NV45E1	45s	15s	NV105E1	105s	15s
NV45E2	45s	15s	NV105E2	105s	15s
NV45E3	45s	15s	NV105E3	105s	15s

A.3 30s break duration experiments

Table A.2 gives the experimental plan for the 30s break duration experiments.

Table A.2: 30s break duration experimental schedule.

Test No.	Break time	Break duration	Test No.	Break time	Break duration
NV00E1	0s	-	NV135E1	135s	30s
NV00E2	0s	-	NV135E2	135s	30s
NV00E3	0s	-	NV135E3	135s	30s
NV15E1	15s	30s	NV150E1	150s	30s
NV15E2	15s	30s	NV150E2	150s	30s
NV15E3	15s	30s	NV150E3	150s	30s
NV30E1	30s	30s	NV165E1	165s	30s
NV30E2	30s	30s	NV165E2	165s	30s
NV30E3	30s	30s	NV165E3	165s	30s
NV45E1	45s	30s	NV180E1	180s	30s
NV45E2	45s	30s	NV180E2	180s	30s
NV45E3	45s	30s	NV180E3	180s	30s
NV60E1	60s	30s	NV195E1	195s	30s
NV60E2	60s	30s	NV195E2	195s	30s
NV60E3	60s	30s	NV195E3	195s	30s
NV75E1	75s	30s	NV210E1	210s	30s
NV75E2	75s	30s	NV210E2	210s	30s
NV75E3	75s	30s	NV210E3	210s	30s
NV90E1	90s	30s	NV225E1	225s	30s
NV90E2	90s	30s	NV225E2	225s	30s
NV90E3	90s	30s	NV225E3	225s	30s
NV105E1	105s	30s	NV240E1	240s	30s
NV105E2	105s	30s	NV240E2	240s	30s
NV105E3	105s	30s	NV240E3	240s	30s
NV120E1	120s	30s	NV120E3	120s	30s
NV120E2	120s	30s			

A.4 60s break duration experiments

The 60s break duration experimental schedule is given in Table A.3.

Table A.3: 60s break duration experimental plan.

Test No.	Break time	Break duration	Test No.	Break time	Break duration
NV00E1	0s	-	NV60E1	60s	60s
NV00E2	0s	-	NV60E2	60s	60s
NV00E3	0s	-	NV60E3	60s	60s
NV15E1	15s	60s	NV75E1	75s	60s
NV15E2	15s	60s	NV75E2	75s	60s
NV15E3	15s	60s	NV75E3	75s	60s
NV30E1	30s	60s	NV90E1	90s	60s
NV30E2	30s	60s	NV90E2	90s	60s
NV30E3	30s	60s	NV90E3	90s	60s
NV45E1	45s	60s	NV105E1	105s	60s
NV45E2	45s	60s	NV105E2	105s	60s
NV45E3	45s	60s	NV105E3	105s	60s

A.5 Repeated break experiments

The planning for the repeated break experiments is given in Table A.4.

Table A.4: Repeated break experimental schedule.

Test No.	Break time	Break duration	Test No.	Break time	Break duration
NV2B80E1	30,110	30s	NV3B100E1	30,130,230	30s
NV2B80E2	30,110	30s	NV3B100E2	30,130,230	30s
NV2B80E3	30,110	30s	NV3B100E3	30,130,230	30s
NV2B150E1	30,180	30s	NV4B30E1	30,90,150,210	30s
NV2B150E2	30,180	30s	NV4B30E2	30,90,150,211	30s
NV2B150E3	30,180	30s	NV4B30E3	30,90,150,212	30s
NV3B80E1	30,110,190	30s	NV3B80E3	30,110,190	30s
NV3B80E2	30,110,190	30s			

EXPERIMENTAL RESULTS

APPENDIX B

B.1 Proximate analysis

A proximate analysis was done, testing for moisture, volatile matter, ash percentage and calorific value. The results of these tests are shown in Tables B.1 – B.4.

Table B.1: The moisture test.

Moisture (SABS 924)				
Sample No.	**Sample mass (g)**	**Final mass (g)**	**Crucible mass (g)**	**% Moisture**
1	1.02	14.08	13.12	5.13
2	1.02	14.01	13.05	5.06
3	1.00	14.00	13.05	5.21
			Ave	5.13

Table B.2: The volatile test.

Volatile matter (ISO 562)				
Sample No.	**Sample mass (g)**	**Final mass (g)**	**Crucible mass (g)**	**% Volatiles**
1	1.0013	13.2862	12.5202	18.37
2	1.0022	14.1667	13.3965	18.09
3	1.0007	13.8512	13.0779	17.52
			Ave	17.99

Table B.3: The ash test.

Ash (ISO 1171)				
Sample No.	**Sample mass (g)**	**Final mass (g)**	**Crucible mass (g)**	**% Ash**
1	1.0022	14.6624	14.1991	46.23
2	1.0176	16.3803	15.9045	46.76
3	1.0035	15.3698	14.9047	46.35
			Ave	46.44

Table B.4: The Calorific value test.

Calorific Value		
Sample No.	**Sample mass (g)**	**CV (kJ/kg)**
1	1.01	12.73
2	1.01	12.71
	Ave	12.72

From this the fixed carbon was calculated as 30.44%.

B.2 Particle size analysis

A particle size analysis was done on five different samples. This also doubles as an accuracy test on the splitting method used. The individual results for each test is shown in Table B.5 – B.9, while the reworked data and an average for each test is shown in Table B.10.

Table B.5: Size analyses: Test 1.

Sieve (μm)	Empty mass (g)	Sieved mass (g)	Gross (g)	Fraction (D)	Fraction (C)
600	500.10	521.10	21.00	0.11	1.00
500	452.90	464.70	11.80	0.06	0.89
425	463.70	468.60	4.90	0.02	0.83
300	466.00	504.20	38.20	0.19	0.81
212	362.10	386.00	23.90	0.12	0.62
150	400.90	421.60	20.70	0.10	0.50
106	467.30	486.70	19.40	0.10	0.40
75	451.50	468.10	16.60	0.08	0.30
0	444.40	486.70	42.30	0.21	0.21
		TOTAL	198.80	1.00	

Table B.6: Size analysis: Test 2.

Sieve (μm)	Empty mass (g)	Sieved mass(g)	Gross (g)	Fraction (D)	Fraction (C)
600	500.10	521.30	21.20	0.11	1.00
500	452.90	467.10	14.20	0.07	0.89
425	463.70	468.50	4.80	0.02	0.82
300	466.00	503.40	37.40	0.19	0.80
212	362.10	390.90	28.80	0.14	0.61
150	400.90	417.10	16.20	0.08	0.47
106	467.30	485.30	18.00	0.09	0.39
75	451.50	463.70	12.20	0.06	0.30
0	444.40	491.00	46.60	0.23	0.23
		TOTAL	199.40	1.00	

Table B.7: Size analysis: Test 3.

Sieve (μm)	Empty mass (g)	Sieved mass (g)	Gross (g)	Fraction (D)	Fraction (C)
600	500.10	520.80	20.70	0.10	1.00
500	452.90	466.40	13.50	0.07	0.90
425	463.70	468.40	4.70	0.02	0.83
300	466.00	497.90	31.90	0.16	0.81
212	362.10	388.90	26.80	0.13	0.65
150	400.90	420.70	19.80	0.10	0.52
106	467.30	493.60	26.30	0.13	0.42
75	451.50	456.80	5.30	0.03	0.29
0	444.40	494.60	50.20	0.25	0.25
		TOTAL	199.20	1.00	

Table B.8: Size analysis: Test 4.

Sieve (μm)	Empty mass (g)	Sieved mass (g)	Gross (g)	Fraction (D)	Fraction (C)
600	500.10	519.90	19.80	0.10	1.00
500	452.90	465.60	12.70	0.06	0.90
425	463.70	468.00	4.30	0.02	0.84
300	466.00	499.90	33.90	0.17	0.82
212	362.10	386.50	24.40	0.12	0.65
150	400.90	420.50	19.60	0.10	0.53
106	467.30	486.30	19.00	0.10	0.43
75	451.50	465.50	14.00	0.07	0.33
0	444.40	496.30	51.90	0.26	0.26
		TOTAL	199.60	1.00	

Table B.9: Size analysis: Test 5.

Sieve (μm)	Empty mass (g)	Sieved mass (g)	Gross (g)	Fraction (D)	Fraction (C)
600	500.10	519.80	19.70	0.10	1.00
500	452.90	466.60	13.70	0.07	0.90
425	463.70	468.10	4.40	0.02	0.83
300	466.00	503.50	37.50	0.19	0.81
212	362.10	392.30	30.20	0.15	0.62
150	400.90	422.70	21.80	0.11	0.47
106	467.30	502.00	34.70	0.17	0.36
75	451.50	462.00	10.50	0.05	0.19
0	444.40	471.30	26.90	0.13	0.13
		TOTAL	199.40	1.00	

Table B.10: Average size fractions.

Sieve (μm)	Cumulative Fractions					
	Test 1	Test 2	Test 3	Test 4	Test 5	Ave
600	1.00	1.00	1.00	1.00	1.00	1.00
500	0.89	0.89	0.90	0.90	0.90	0.90
425	0.83	0.82	0.83	0.84	0.83	0.83
300	0.81	0.80	0.81	0.82	0.81	0.81
212	0.62	0.61	0.65	0.65	0.62	0.63
150	0.50	0.47	0.52	0.53	0.47	0.50
106	0.40	0.39	0.42	0.43	0.36	0.40
75	0.30	0.30	0.29	0.33	0.19	0.28
0	0.21	0.23	0.25	0.26	0.13	0.22

The graph of the particle size analysis is shown as Figure 3.4 (§3.3.2).

B.3 15s break duration test results

The data given for each group of experiments in Table B.11 is an average of three tests per group and just every tenth point. For more detailed data see the attached CD.

Table B.11: 15s break duration moisture fractions.

	Moisture fractions							
Time (s)	**No break**	**15s**	**30s**	**45s**	**60s**	**75s**	**90s**	**105s**
0	0.423	0.431	0.419	0.408	0.410	0.414	0.416	0.415
1	0.420	0.423	0.416	0.408	0.407	0.409	0.408	0.412
10	0.378	0.387	0.383	0.371	0.366	0.375	0.370	0.366
20	0.351	0.358	0.356	0.347	0.346	0.354	0.343	0.345
30	0.341	0.347	0.342	0.343	0.342	0.336	0.336	0.323
40	0.333	0.351	0.342	0.333	0.339	0.336	0.336	0.319
50	0.337	0.333	0.342	0.329	0.335	0.329	0.332	0.315
60	0.337	0.315	0.338	0.329	0.335	0.325	0.328	0.311
70	0.337	0.306	0.335	0.333	0.335	0.325	0.324	0.315
80	0.333	0.303	0.331	0.329	0.331	0.321	0.324	0.303
90	0.333	0.294	0.323	0.321	0.331	0.321	0.324	0.307
100	0.330	0.294	0.323	0.325	0.328	0.325	0.320	0.298
110	0.333	0.290	0.315	0.321	0.324	0.317	0.324	0.302
120	0.329	0.286	0.319	0.321	0.320	0.317	0.320	0.306
130	0.329	0.282	0.319	0.317	0.320	0.313	0.317	0.298
140	0.326	0.282	0.316	0.317	0.320	0.313	0.313	0.298
150	0.330	0.282	0.312	0.317	0.312	0.305	0.317	0.290
160	0.330	0.282	0.316	0.317	0.316	0.309	0.313	0.294
170	0.326	0.278	0.312	0.313	0.312	0.305	0.313	0.291
180	0.330	0.273	0.311	0.313	0.308	0.305	0.313	0.291
190	0.326	0.278	0.311	0.313	0.308	0.305	0.313	0.294
200	0.326	0.278	0.312	0.309	0.308	0.305	0.313	0.286
210	0.330	0.273	0.316	0.310	0.308	0.305	0.309	0.291
220	0.326	0.269	0.312	0.310	0.308	0.305	0.305	0.286
230	0.326	0.273	0.311	0.309	0.308	0.301	0.305	0.286
240	0.326	0.264	0.308	0.309	0.308	0.305	0.305	0.282
250	0.326	0.269	0.312	0.310	0.308	0.301	0.305	0.286
260	0.326	0.269	0.304	0.313	0.304	0.305	0.305	0.286
270	0.326	0.269	0.316	0.313	0.308	0.297	0.301	0.282
280	0.326	0.269	0.312	0.310	0.308	0.309	0.305	0.282
290	0.326	0.269	0.312	0.309	0.308	0.301	0.301	0.286

300	0.326	0.260	0.304	0.306	0.300	0.293	0.301	0.286

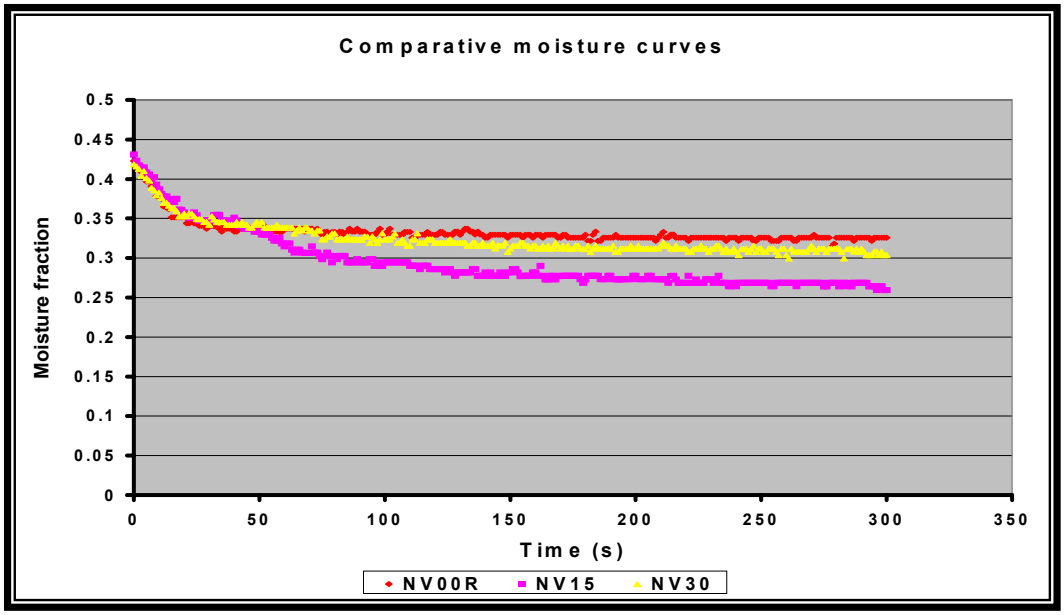

Figure B.1: 15s break duration results.

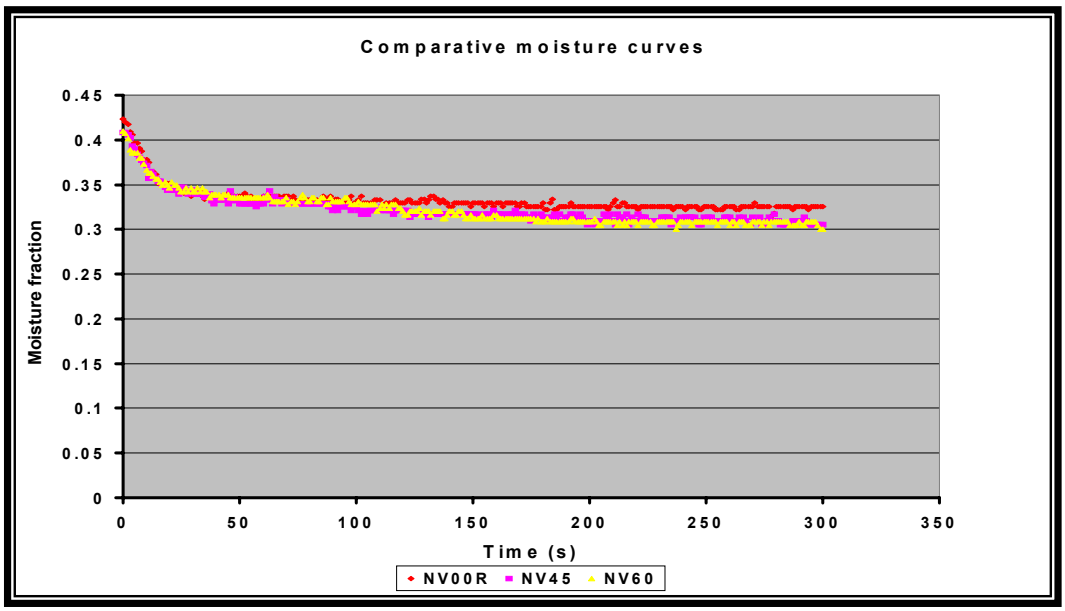

Figure B.2: 15s break duration results.

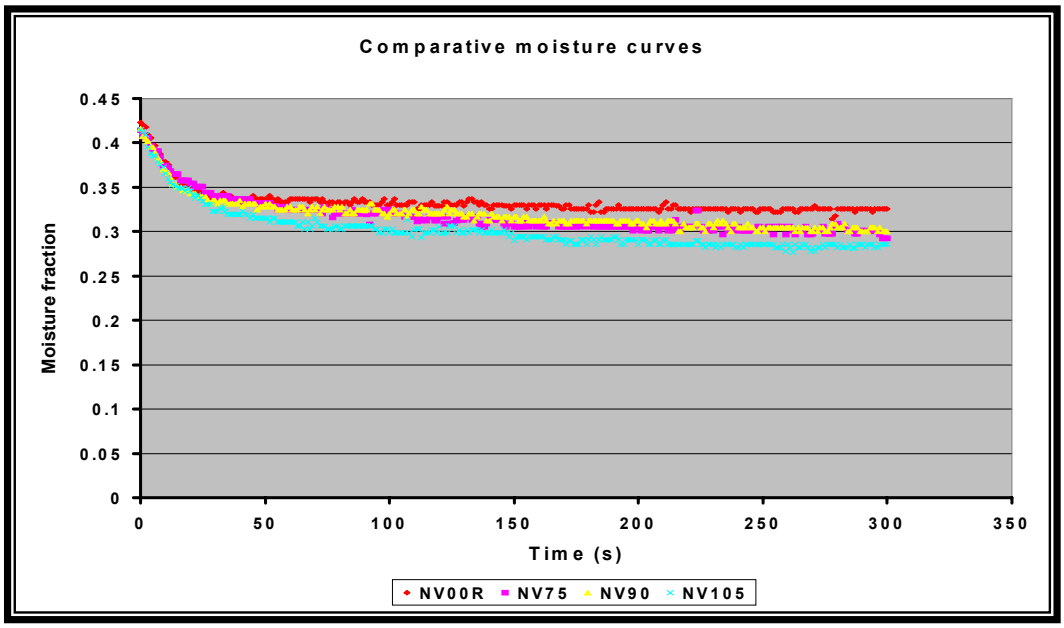

Figure B.3: 15s break duration results.

B.4 30s break duration results

The data given below for each group of experiments in Table B.12 and Table B.13, is an average of three tests per group. Also it is given for every tenth point only. For more detailed data see the attached CD.

Table B.12: 30s break duration moisture fractions.

	Moisture fractions								
Time(s)	No Break	15s	30s	45s	60s	75s	90s	105s	120s
0	0.423	0.383	0.451	0.423	0.441	0.454	0.416	0.454	0.430
1	0.420	0.378	0.443	0.419	0.436	0.454	0.413	0.451	0.421
10	0.378	0.358	0.392	0.368	0.403	0.409	0.374	0.423	0.391
20	0.351	0.308	0.356	0.325	0.370	0.367	0.347	0.388	0.372
30	0.341	0.290	0.316	0.302	0.350	0.341	0.336	0.369	0.372
40	0.333	0.290	0.304	0.296	0.350	0.330	0.336	0.354	0.362
50	0.337	0.290	0.304	0.289	0.345	0.324	0.336	0.349	0.367
60	0.337	0.284	0.300	0.289	0.339	0.324	0.332	0.349	0.362
70	0.337	0.284	0.308	0.283	0.350	0.324	0.332	0.343	0.362
80	0.333	0.271	0.300	0.270	0.339	0.324	0.325	0.343	0.362
90	0.333	0.264	0.296	0.283	0.345	0.319	0.332	0.343	0.362
100	0.330	0.264	0.288	0.276	0.350	0.318	0.328	0.338	0.362
110	0.333	0.257	0.279	0.277	0.345	0.312	0.328	0.338	0.362
120	0.329	0.257	0.279	0.277	0.339	0.312	0.325	0.343	0.356
130	0.329	0.257	0.275	0.270	0.334	0.307	0.328	0.343	0.362
140	0.326	0.257	0.275	0.270	0.323	0.301	0.317	0.343	0.362
150	0.330	0.264	0.270	0.270	0.328	0.301	0.313	0.338	0.362
160	0.330	0.257	0.270	0.270	0.323	0.289	0.317	0.332	0.362
170	0.326	0.257	0.257	0.270	0.323	0.295	0.309	0.327	0.356
180	0.330	0.257	0.261	0.270	0.323	0.295	0.301	0.327	0.346
190	0.326	0.257	0.257	0.256	0.323	0.295	0.309	0.327	0.346
200	0.326	0.257	0.252	0.270	0.317	0.289	0.297	0.327	0.346
210	0.330	0.257	0.257	0.256	0.311	0.282	0.305	0.327	0.335
220	0.326	0.257	0.257	0.263	0.311	0.295	0.301	0.321	0.340
230	0.326	0.257	0.252	0.263	0.317	0.295	0.301	0.321	0.335
240	0.326	0.257	0.252	0.256	0.311	0.289	0.301	0.315	0.335
250	0.326	0.257	0.252	0.263	0.317	0.282	0.301	0.321	0.335
260	0.326	0.257	0.252	0.263	0.317	0.289	0.305	0.315	0.335
270	0.326	0.257	0.252	0.263	0.317	0.282	0.297	0.321	0.335
280	0.326	0.257	0.252	0.263	0.317	0.282	0.305	0.321	0.329
290	0.326	0.257	0.252	0.263	0.317	0.282	0.305	0.309	0.329
300	0.326	0.263	0.252	0.274	0.302	0.292	0.305	0.301	0.315

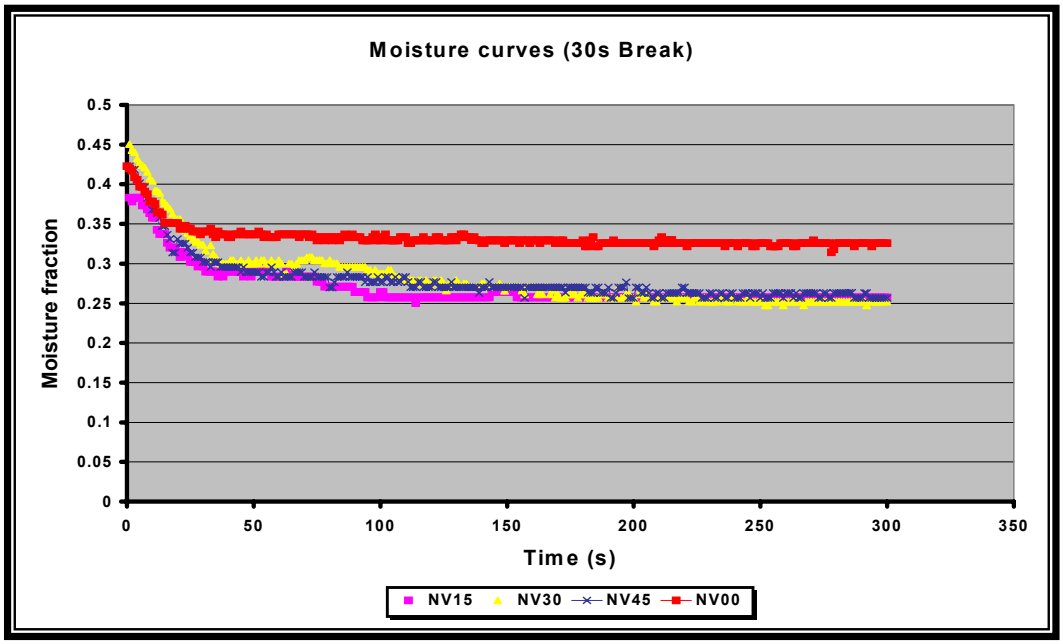

Figure B.4: 30s break duration results.

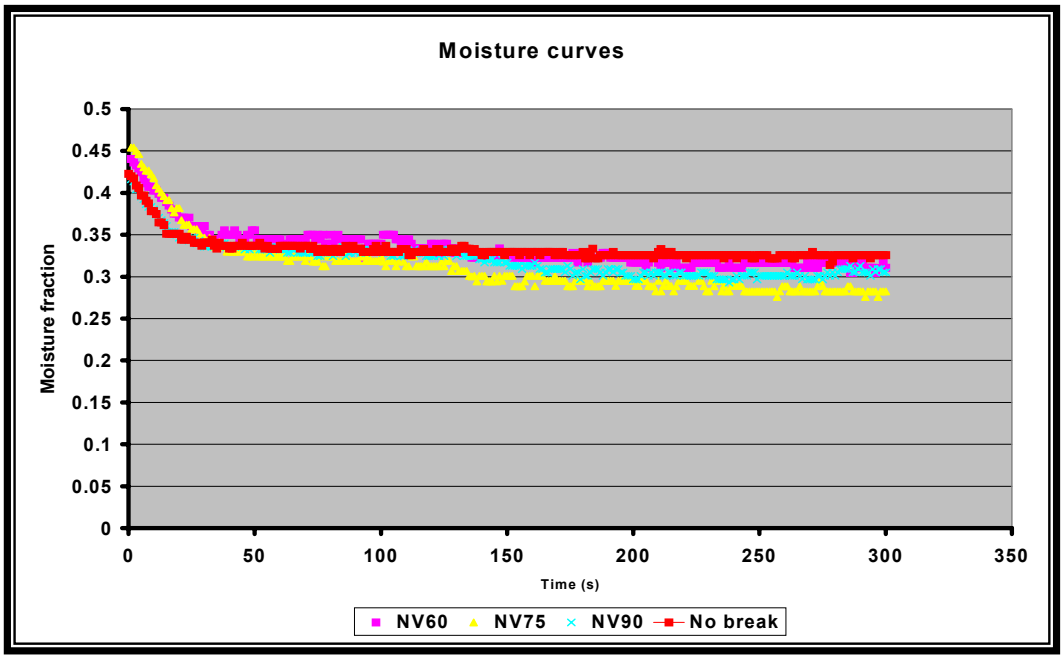

Figure B.5: 30 break duration results.

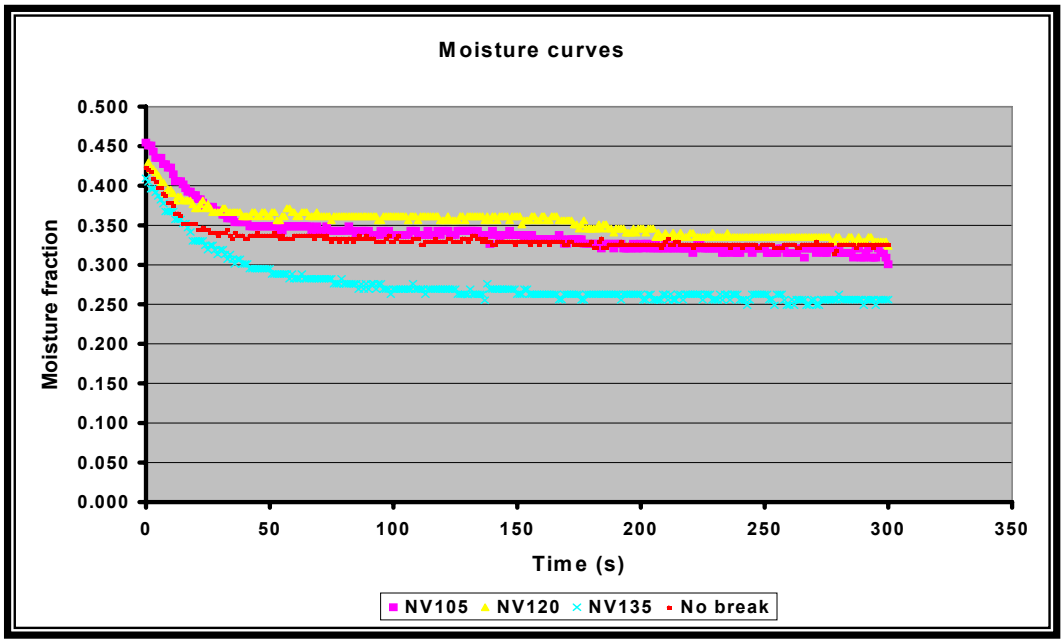

Figure B.6: 30s break duration results.

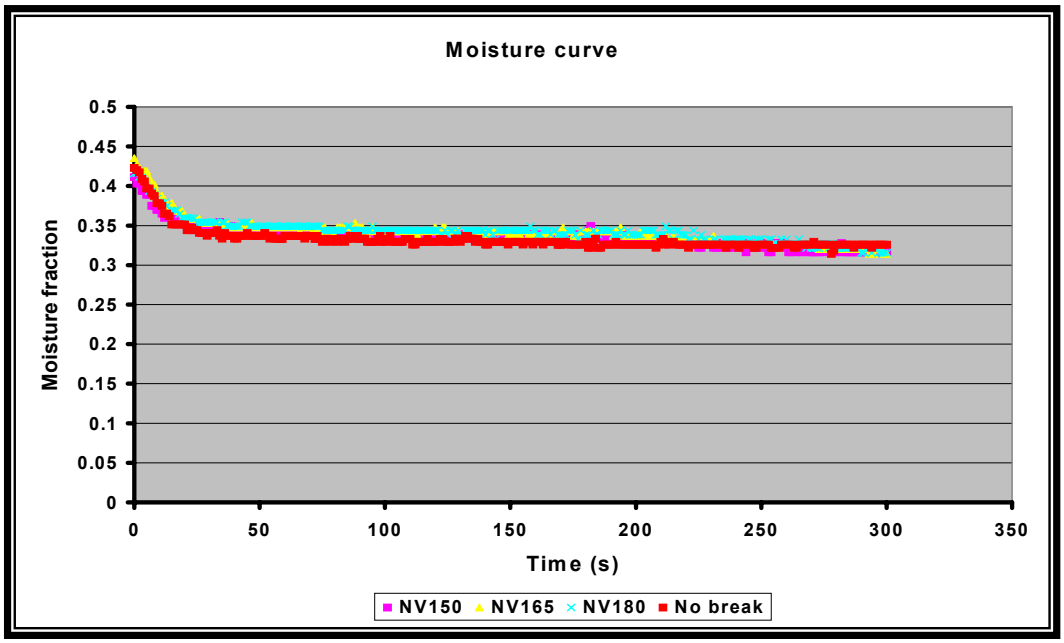

Figure B.7: 30s break duration results.

Table B.13: 30s break duration moisture fractions.

	Moisture fractions								
Time(s)	No Break	135s	150s	165s	180s	195s	210s	225s	240s
0	0.423	0.409	0.411	0.435	0.416	0.434	0.407	0.416	0.433
1	0.420	0.405	0.403	0.427	0.416	0.426	0.407	0.408	0.425
10	0.378	0.368	0.370	0.388	0.379	0.388	0.370	0.375	0.387
20	0.351	0.330	0.355	0.364	0.359	0.365	0.349	0.350	0.357
30	0.341	0.319	0.350	0.353	0.354	0.348	0.342	0.323	0.350
40	0.333	0.301	0.344	0.348	0.349	0.348	0.342	0.305	0.350
50	0.337	0.295	0.339	0.348	0.349	0.348	0.338	0.293	0.343
60	0.337	0.282	0.339	0.348	0.349	0.348	0.331	0.293	0.343
70	0.337	0.282	0.339	0.348	0.349	0.341	0.331	0.286	0.343
80	0.333	0.276	0.339	0.337	0.344	0.341	0.331	0.273	0.343
90	0.333	0.269	0.339	0.348	0.344	0.341	0.331	0.273	0.343
100	0.330	0.269	0.339	0.337	0.344	0.341	0.331	0.273	0.343
110	0.333	0.269	0.339	0.337	0.344	0.341	0.331	0.273	0.343
120	0.329	0.269	0.339	0.348	0.344	0.341	0.331	0.273	0.339
130	0.329	0.262	0.339	0.337	0.338	0.337	0.331	0.267	0.336
140	0.326	0.269	0.339	0.343	0.338	0.341	0.331	0.267	0.339
150	0.330	0.263	0.333	0.337	0.344	0.337	0.331	0.260	0.339
160	0.330	0.263	0.339	0.337	0.344	0.337	0.327	0.260	0.336
170	0.326	0.263	0.339	0.343	0.338	0.341	0.331	0.260	0.335
180	0.330	0.263	0.339	0.343	0.338	0.337	0.327	0.260	0.335
190	0.326	0.263	0.339	0.343	0.344	0.337	0.327	0.260	0.332
200	0.326	0.263	0.328	0.337	0.338	0.337	0.331	0.267	0.332
210	0.330	0.263	0.328	0.332	0.338	0.337	0.327	0.260	0.335
220	0.326	0.263	0.328	0.337	0.338	0.344	0.327	0.267	0.335
230	0.326	0.256	0.328	0.332	0.327	0.337	0.327	0.260	0.335
240	0.326	0.256	0.328	0.326	0.333	0.333	0.331	0.260	0.332
250	0.326	0.263	0.328	0.326	0.333	0.329	0.331	0.260	0.328
260	0.326	0.249	0.322	0.326	0.333	0.330	0.327	0.266	0.325
270	0.326	0.256	0.316	0.326	0.321	0.322	0.320	0.260	0.325
280	0.326	0.263	0.316	0.320	0.321	0.318	0.316	0.253	0.325
290	0.326	0.249	0.316	0.320	0.316	0.318	0.312	0.260	0.317
300	0.326	0.256	0.316	0.314	0.316	0.318	0.308	0.253	0.317

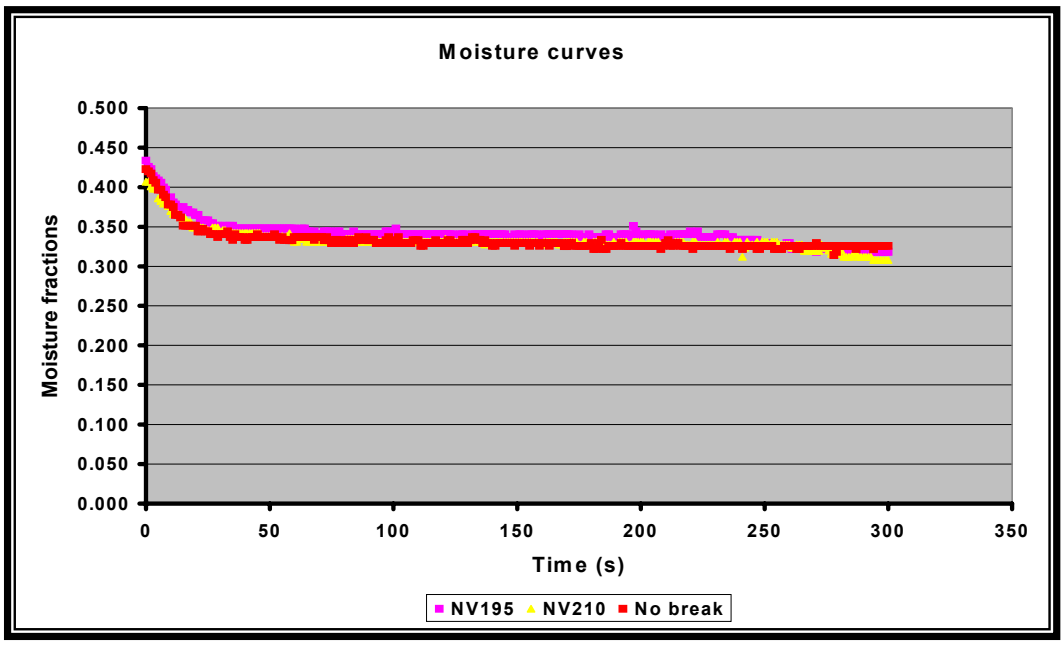

Figure B.8: 30s break duration results.

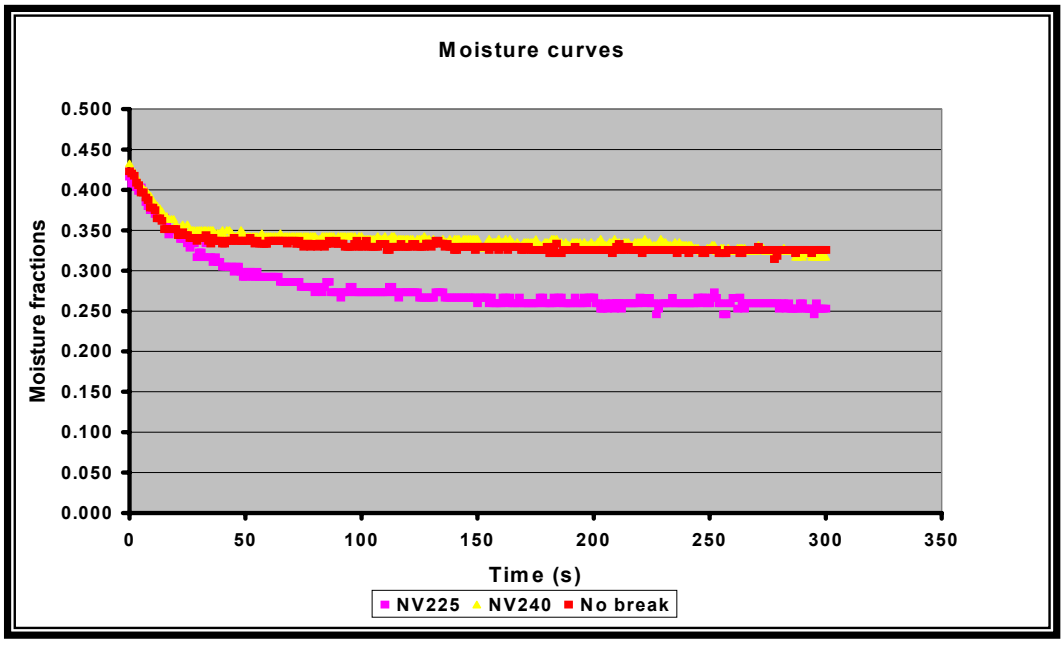

Figure B.9: 30s break duration results.

B.5 60s break duration results

The data given for each group of experiments in Table B.14 is an average of three tests per group and just every tenth point. For more detailed data see the attached CD.

Table B.14: 60s break duration moisture fractions.

	Moisture fractions							
Time (s)	**No break**	**15s**	**30s**	**45s**	**60s**	**75s**	**90s**	**105s**
0	0.423	0.410	0.427	0.408	0.436	0.438	0.452	0.421
1	0.420	0.407	0.419	0.402	0.431	0.430	0.447	0.416
10	0.378	0.366	0.373	0.361	0.381	0.380	0.382	0.376
20	0.351	0.346	0.343	0.344	0.351	0.354	0.362	0.353
30	0.341	0.342	0.336	0.344	0.348	0.347	0.345	0.339
40	0.333	0.339	0.336	0.344	0.348	0.343	0.341	0.328
50	0.337	0.335	0.336	0.339	0.344	0.339	0.334	0.328
60	0.337	0.335	0.336	0.329	0.337	0.339	0.334	0.324
70	0.337	0.335	0.332	0.329	0.341	0.336	0.326	0.320
80	0.333	0.331	0.329	0.329	0.341	0.328	0.330	0.316
90	0.333	0.331	0.336	0.329	0.341	0.332	0.322	0.316
100	0.330	0.328	0.332	0.329	0.341	0.332	0.322	0.316
110	0.333	0.324	0.321	0.329	0.341	0.336	0.322	0.312
120	0.329	0.320	0.310	0.329	0.341	0.332	0.326	0.320
130	0.329	0.320	0.310	0.322	0.341	0.332	0.322	0.316
140	0.326	0.320	0.297	0.322	0.333	0.332	0.322	0.308
150	0.330	0.312	0.297	0.318	0.330	0.332	0.322	0.311
160	0.330	0.316	0.293	0.318	0.322	0.328	0.322	0.308
170	0.326	0.312	0.289	0.314	0.322	0.328	0.326	0.311
180	0.330	0.308	0.289	0.314	0.314	0.325	0.314	0.308
190	0.326	0.308	0.293	0.310	0.314	0.321	0.311	0.308
200	0.326	0.308	0.289	0.310	0.310	0.321	0.307	0.299
210	0.330	0.308	0.289	0.310	0.310	0.317	0.307	0.304
220	0.326	0.308	0.289	0.310	0.310	0.321	0.307	0.299
230	0.326	0.308	0.285	0.310	0.310	0.317	0.307	0.299
240	0.326	0.308	0.289	0.302	0.314	0.321	0.307	0.295
250	0.326	0.308	0.289	0.306	0.310	0.313	0.307	0.304
260	0.326	0.304	0.285	0.310	0.306	0.317	0.307	0.299
270	0.326	0.308	0.285	0.306	0.310	0.313	0.303	0.292
280	0.326	0.308	0.285	0.306	0.306	0.313	0.307	0.299
290	0.326	0.308	0.289	0.302	0.310	0.313	0.307	0.295
300	0.326	0.300	0.289	0.306	0.310	0.313	0.303	0.292

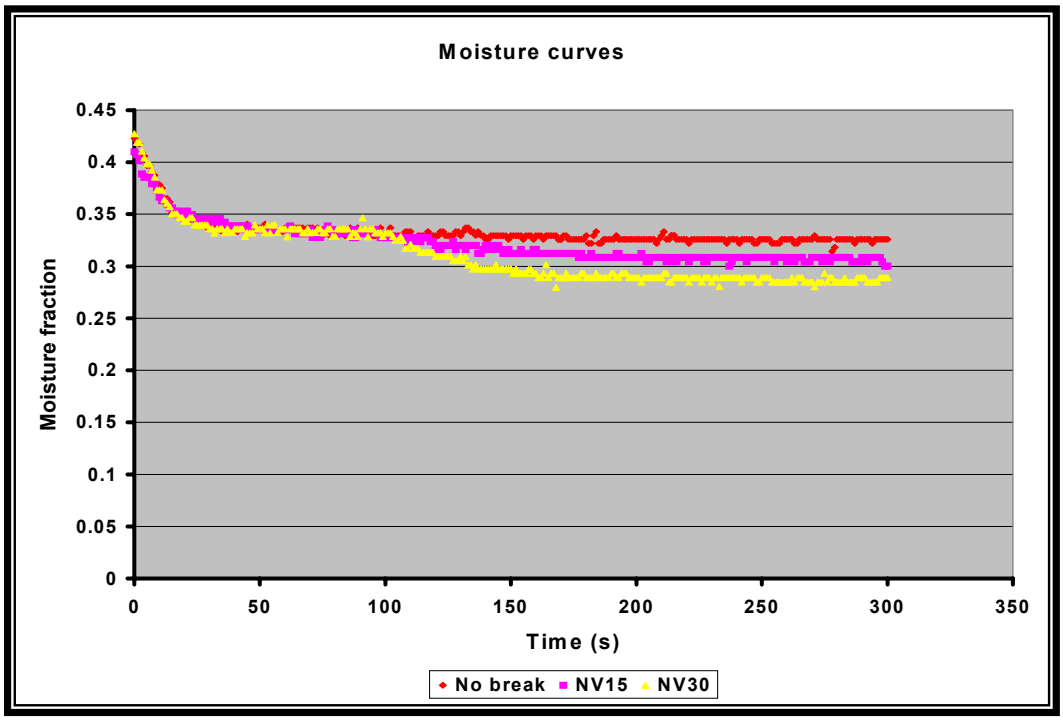

Figure B.10: 60s break duration results.

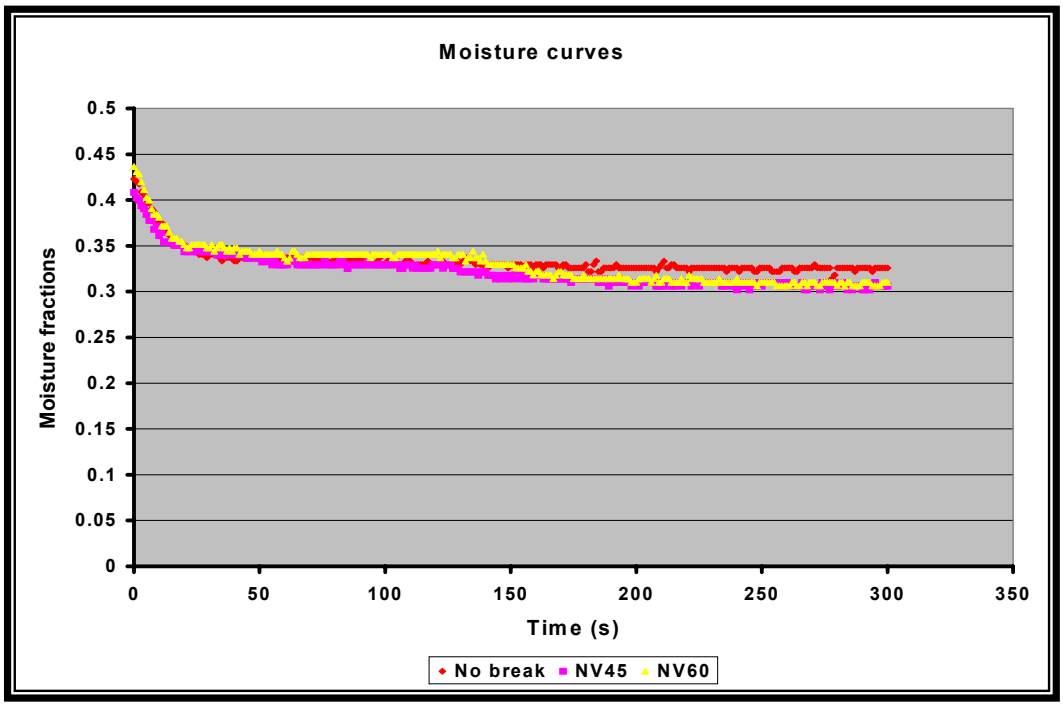

Figure B.11: 60s break duration results.

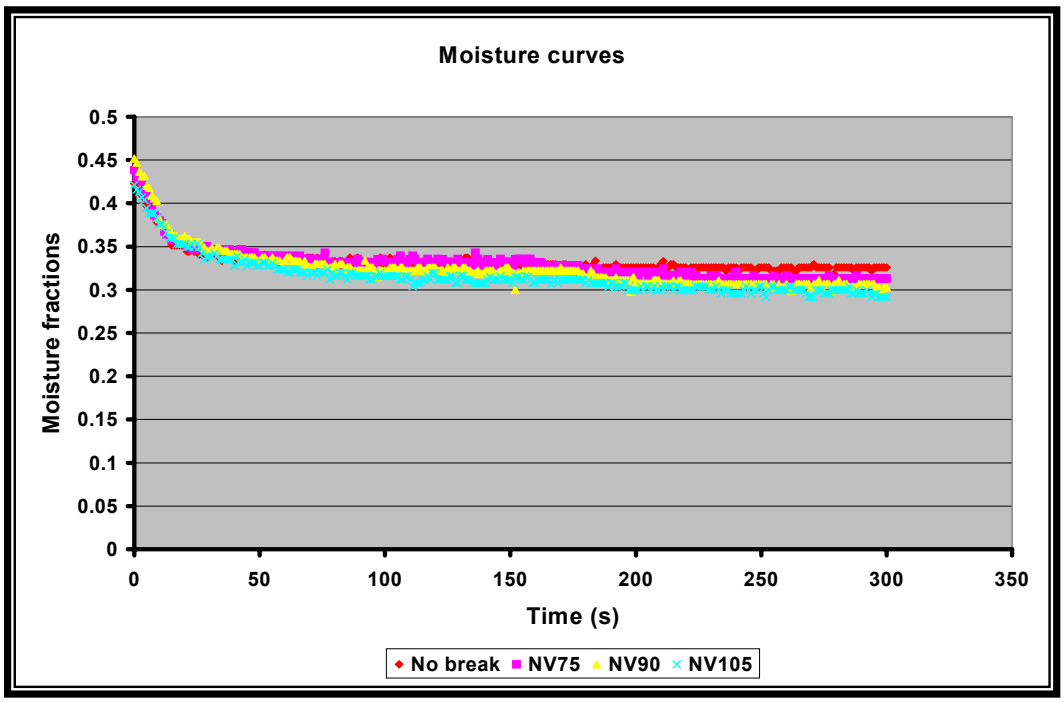

Figure B.12: 60s break duration results.

B.6 Cake break test results

The data given below for each group of experiments in Table B.15, is an average of three tests per group. Also it is given for every tenth point only. For more detailed data see the attached CD.

Table B.15: Cake break test moisture fractions.

	Moisture fractions		
Time (s)	No break	Cake break	30s break
0	0.423	0.397	0.451
1	0.420	0.394	0.451
10	0.378	0.362	0.404
20	0.351	0.338	0.356
30	0.341	0.331	0.324
40	0.333	0.291	0.300
50	0.337	0.278	0.300
60	0.337	0.274	0.304
70	0.337	0.270	0.304
80	0.333	0.270	0.304
90	0.333	0.265	0.296
100	0.330	0.265	0.288
110	0.333	0.270	0.279
120	0.329	0.265	0.270
130	0.329	0.261	0.279
140	0.326	0.265	0.275
150	0.330	0.261	0.270
160	0.330	0.261	0.270
170	0.326	0.265	0.261
180	0.330	0.265	0.261
190	0.326	0.261	0.257
200	0.326	0.261	0.257
210	0.330	0.256	0.257
220	0.326	0.261	0.257
230	0.326	0.265	0.252
240	0.326	0.261	0.257
250	0.326	0.261	0.252
260	0.326	0.256	0.252
270	0.326	0.261	0.252
280	0.326	0.261	0.252
290	0.326	0.256	0.252
300	0.326	0.265	0.252

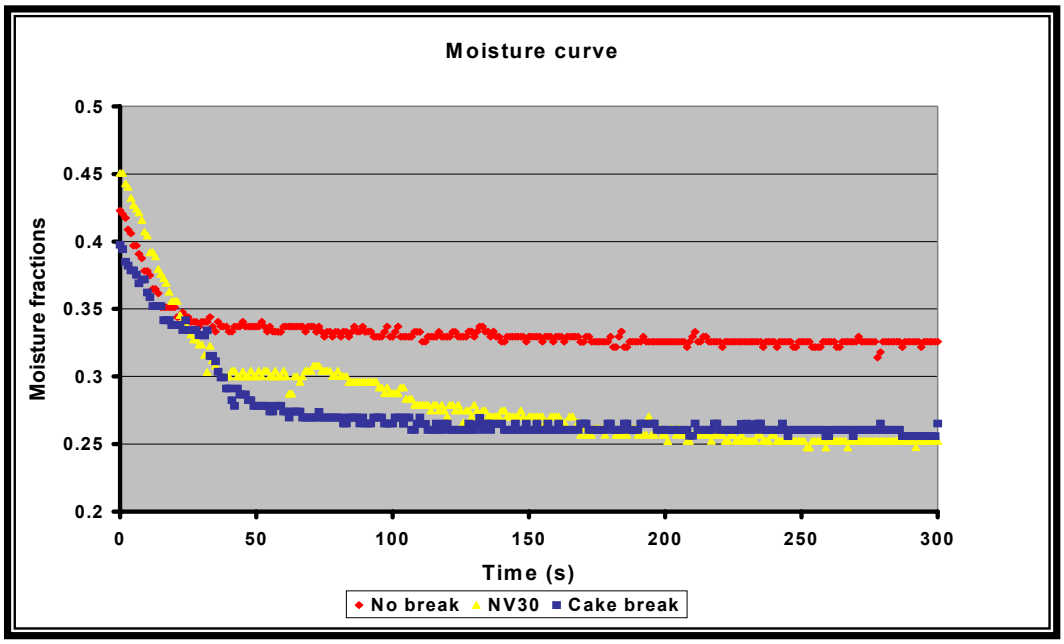

Figure B.13: Cake break test results.

B.7 Repeated break test results

The data given below for each group of experiments in Table B.16, is an average of three tests per group. Also it is given for every tenth point only. For more detailed data see the attached CD.

Table B.16: Repeated break test moisture fractions.

	Moisture fractions				
Time(s)	**No break**	**2B80**	**2B150**	**3B80**	**3B100**
0	0.423	0.435	0.429	0.405	0.437
1	0.420	0.432	0.421	0.398	0.429
10	0.378	0.379	0.372	0.354	0.382
20	0.351	0.353	0.355	0.330	0.339
30	0.341	0.346	0.352	0.322	0.328
40	0.333	0.342	0.352	0.311	0.320
50	0.337	0.339	0.352	0.311	0.316
60	0.337	0.339	0.348	0.311	0.312
70	0.337	0.342	0.348	0.311	0.324
80	0.333	0.339	0.341	0.311	0.312
90	0.333	0.328	0.341	0.303	0.308
100	0.330	0.328	0.341	0.299	0.308
110	0.333	0.324	0.334	0.299	0.308
120	0.329	0.312	0.330	0.294	0.300
130	0.329	0.316	0.330	0.294	0.312
140	0.326	0.320	0.327	0.294	0.296
150	0.330	0.320	0.327	0.294	0.308
160	0.330	0.320	0.327	0.294	0.300
170	0.326	0.316	0.323	0.294	0.296
180	0.330	0.316	0.319	0.299	0.292
190	0.326	0.312	0.319	0.290	0.292
200	0.326	0.308	0.327	0.286	0.296
210	0.330	0.308	0.327	0.294	0.292
220	0.326	0.304	0.327	0.294	0.296
230	0.326	0.308	0.323	0.294	0.292
240	0.326	0.308	0.323	0.294	0.292
250	0.326	0.304	0.315	0.294	0.296
260	0.326	0.308	0.319	0.290	0.300
270	0.326	0.308	0.319	0.290	0.296
280	0.326	0.304	0.315	0.286	0.292
290	0.326	0.300	0.315	0.286	0.296
300	0.326	0.304	0.307	0.290	0.300

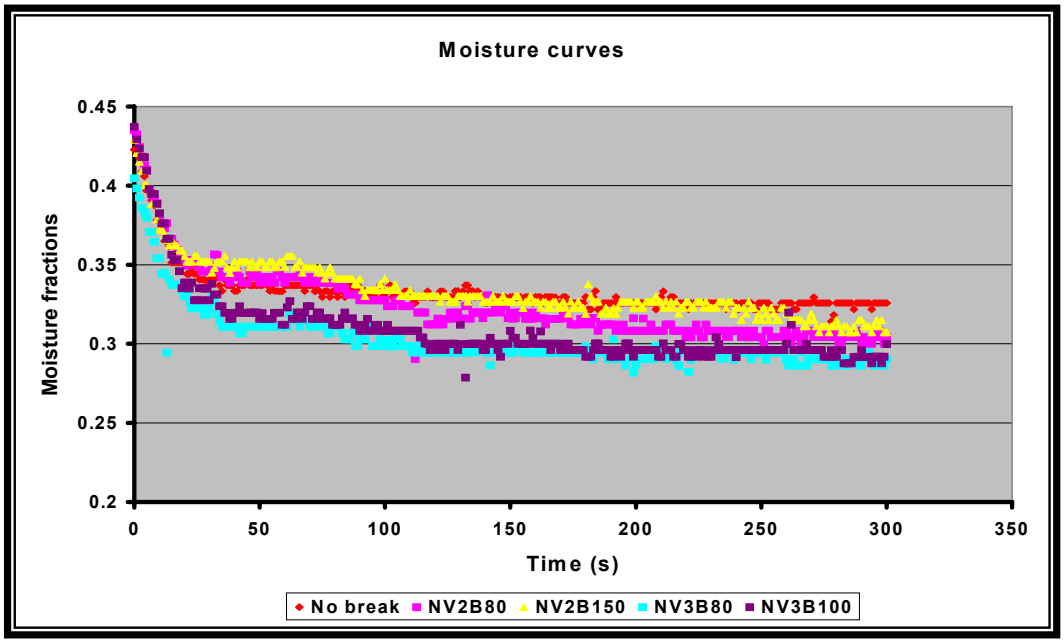

Figure B.14: Repeated break test results.

SAMPLE CALCULATIONS

APPENDIX C

C.1 Moisture calculations

For a sample calculation, the calculations for the first experiment, and the first second thereof, are shown below. The data that was recorded on the computer is shown in Table C.1. Note again that the data is only given for every tenth point. To view all the data, see the attached CD.

In addition to the data in Table C.1, the following information was also necessary.

Cake mass after dewatering (M_{cw}) = 121.20g.

Cake mass after thermal drying (M_{cd}) = 107.70g.

Mass water pulled from the cake after 100% saturation (M_w) = 31.50g.

Mass solids (M_s) = 40.00g.

- The first step was to convert the mass filtrate (M_f) from kg to g. This was done by calculation C.1.

$$\begin{aligned} M_f &= M_{fc} \cdot 1000 \\ &= 0.001 \cdot 1000 \\ &= 1\text{g} \end{aligned} \qquad \text{(C.1)}$$

with M_{fc} the mass filtrate as read from the computer.

- The second step was to determine the moisture fraction in the filter cake at any given time. This was done, using calculation C.2.

$$\begin{aligned} \text{Moisture fraction} &= \frac{M_w - M_f}{M_s + M_w + M_f} \\ &= \frac{31.5 - 1}{40 + 31.5 - 1} \\ &= 0.433 \end{aligned} \qquad \text{(C.2)}$$

Table C.1: Sample calculations.

Vacuum (kPa)	Mass (kg)	Time (s)	New Mass (g)	Moisture fraction
45.17	0.000	0	0.00	0.441
45.17	0.001	1	1.00	0.433
45.15	0.007	10	7.00	0.380
45.14	0.011	20	11.00	0.339
45.15	0.014	30	14.00	0.304
0.00	0.014	40	14.00	0.304
0.00	0.014	50	14.00	0.304
0.00	0.015	60	15.00	0.292
32.00	0.014	70	14.00	0.304
39.42	0.014	80	14.00	0.304
41.15	0.014	90	14.00	0.304
41.47	0.015	100	15.00	0.292
41.79	0.015	110	15.00	0.292
42.70	0.015	120	15.00	0.292
44.13	0.016	130	16.00	0.279
44.33	0.015	140	15.00	0.292
44.77	0.016	150	16.00	0.279
44.59	0.016	160	16.00	0.279
44.49	0.017	170	17.00	0.266
44.34	0.017	180	17.00	0.266
44.40	0.017	190	17.00	0.266
45.66	0.017	200	17.00	0.266
45.85	0.017	210	17.00	0.266
45.85	0.017	220	17.00	0.266
45.85	0.018	230	18.00	0.252
45.78	0.018	240	18.00	0.252
45.74	0.018	250	18.00	0.252
45.71	0.018	260	18.00	0.252
45.65	0.018	270	18.00	0.252
45.60	0.018	280	18.00	0.252
45.54	0.018	290	18.00	0.252
45.53	0.018	300	18.00	0.252

WAKEMAN'S ALGORITHM

APPENDIX D

D.1 General

Dr. Richard Wakeman created an algorithm for the solving of his dewatering model. The algorithm is given below (taken from Wakeman, 1978).

For computational purposes the cake was divided into a number of elemental slices, and the initial pressure and saturation conditions were calculated for each layer. Computations were started at the free cake surface where the input rate of residual filtrate was zero, and after a time interval $\Delta\theta$ a 'front' of air was considered to have moved through a layer of thickness $\Delta(x/L)$. During this frontal displacement some of the residual filtrate was displaced into the next successive distance increment, and from the final increment some liquid was displaced from the cake. The filtrate flow rate was calculable from Equation 2.23 in the form:

$$\upsilon^{*}_{L_{x+1/2,t}} = -S^{(2+3\lambda)/\lambda}_{R_{x+1/2,t}} \frac{P^{*}_{L_{x+1,t}} - P^{*}_{L_{x,t}}}{\Delta(x/L)} \qquad (D.1)$$

The change of saturation of each layer was governed by the filtrate material balance, Equation 2.25 , from which the new saturation of each layer was obtained:

$$S_{R_{x,t+1}} = S_{R_{x,t}} - \frac{\Delta\theta}{\Delta(x/L)}\left[\upsilon^{*}_{L_{x+1,t}} - \upsilon^{*}_{L_{x,t}}\right] \qquad (D.2)$$

The airflow into each layer was then given by an air mass balance over each slice of cake:

$$\upsilon^{*}_{a_{x,t}} = \frac{\rho_{a_{x+1,t}}}{\rho_{a_{x,t}}}\upsilon^{*}_{a_{x+1,t}} + \frac{\mu_a}{\mu_L}\frac{\Delta(x/L)}{\Delta\theta}\left[\frac{\rho_{a_{x,t+1}}}{\rho_{a_{x,t}}}\left(1 - S_{R_{x,t+1}}\right) - \left(1 - S_{R_{x,t}}\right)\right] \qquad (D.3)$$

where dewatering was assumed to be isothermal, hence

$$\frac{\rho_{a_1}}{\rho_{a_2}} = \frac{P_{a_1}}{P_{a_2}} = \frac{P^*_{a_1}}{P^*_{a_2}} \tag{D.4}$$

After air breakthrough the air rate from the cake was unknown. This value was estimated in order to use Equation D.4, and after calculation of the air pressure profile from Equation 2.24 in the form:

$$P^*_{a_{x+1,t}} = P^*_{a_{x,t}} - \frac{\upsilon^*_{a_{x+1/2,t}} \Delta(x/L)}{\left(1 - S_{R_{x+1/2,t}}\right)^2 \left(1 - S^{(2+\lambda)/\lambda}_{R_{x+1/2,t}}\right)} \tag{D.5}$$

The pressure at the bed outlet was compared with the experimental values correlated by Equation 2.6. Repeated calculations of $\upsilon^*_{a_{x,t}}$ and $P^*_{a_{x+1,t}}$ were made, adjusting the air rate from the cake, until agreement between computed and experimental results was obtained. The liquid pressure profile at the start of the next time increment could be calculated from Equation 2.27 as:

$$P^*_{L_{x,t}} = P^*_{a_{w,t}} - S^{-1/\lambda}_{R_{x,t}} \tag{D.6}$$

Stability criteria for the system of Equations D.1-D.3 and D.5 were difficult to obtain analytically. Preliminary assessment of the model was done by computing dewatering curves at constant total pressure drop. Consistent results were obtained by dividing the cake into j layers where the maximum number of layers was defined by:

$$j_{\max} = \left[\Delta P^*\right]_{t=0} - 1 \tag{D.7}$$

where $[\Delta P^*]$ was the integer whose magnitude did not exceed the magnitude of the initial total pressure drop ΔP^* across the bed, hence:

$$\Delta(x/L) = 1/j_{\max} \tag{D.8}$$

This distance increment was held constant for all time increments, whose magnitude varied according to the conditions in the saturated part of the bed immediately ahead of the advancing front:

$$\frac{\Delta\theta}{\left(\Delta(x/L)\right)^2} = 0.25 / \left(P^*_{L_i} - P^*_{L_{i+1}}\right) \tag{D.9}$$

where subscript *i* denoted the node point in the cake reached by the front. After air breakthrough $\Delta\theta$ was constant for the remainder of the computations. It is recognised that this scheme might be impractical if $[\Delta P^*] < 2$, but this would represent an extraordinarily unusual situation in filter cake dewatering.